

University of Leipzig  
Leipzig Institute for Meteorology  
Leibniz Institute for Tropospheric Research

Bachelor Thesis

**Observation and RT-Modelling of Spectrally  
Resolved UV-Radiation in Melpitz, Germany**

**Author:** Nicolas Bayer

**Matriculation Number:** 3736946

**1st Reviewer:** Andreas Macke

**2nd Reviewer:** Hartwig Deneke

**Submission Date:** 20. October 2020



# Contents

<b>1</b>	<b>Introduction</b>	<b>1</b>
<b>2</b>	<b>Methods</b>	<b>4</b>
2.1	Radiation . . . . .	4
2.2	Measuring Station Melpitz . . . . .	4
2.3	Cams Reanalysis Data Set . . . . .	5
2.4	The Ultraviolet Index (UVI) . . . . .	6
2.5	Important Factors Influencing the UVI . . . . .	6
2.5.1	Solar Zenith Angle (SZA) . . . . .	7
2.5.2	Total Ozone Column (TOZ) . . . . .	7
2.5.3	Clouds . . . . .	8
2.5.4	Surface Albedo . . . . .	8
2.5.5	Aerosol Optical Depth (AOD) . . . . .	8
2.5.6	Altitude . . . . .	9
2.6	Radiative Transfer Model . . . . .	10
<b>3</b>	<b>Sensitivity Studies</b>	<b>12</b>
3.1	LibRadtran Model Configuration's Inputs Sensitivity Study . . . . .	12
3.2	Meteorological Inputs Sensitivity study . . . . .	13
3.2.1	Total Column Ozone . . . . .	13
3.2.2	Surface Albedo . . . . .	15
3.2.3	Aerosol Optical Depth . . . . .	16
<b>4</b>	<b>Comparison of RT Simulations and Observations</b>	<b>19</b>
4.1	Cases Studies . . . . .	19
4.2	Results . . . . .	19
<b>5</b>	<b>Conclusion and Outlook</b>	<b>25</b>
5.1	Conclusions . . . . .	25
5.2	Outlook . . . . .	27
<b>Appendix</b>		<b>vi</b>



# Chapter 1

## Introduction

The solar radiation is the energy emitted by the sun in the form of electromagnetic waves. The sun is the main source of energy for the Earth. It emits a variety of wavelengths, including ultraviolet radiation (100-400 nm), visible spectrum (400-700 nm), and infrared (700- nm-4μm).

This thesis will focus on the UV radiation, which is further divided into three bands: UV-A (315-400 nm), UV-B (280-315 nm) and UV-C (100-280 nm)(WHO, 1995). As UV radiation passes through the atmosphere, water vapor, oxygen, ozone and carbon dioxide absorb all UV-C and approximately 90% of UV-B radiation. The amount of UV-B that reaches the surface, anti-correlated the amount of ozone present in the atmosphere. Therefore, the UV radiation that reaches the earth's surface is mostly composed of UV-A radiation, with a small amount of UV-B radiation.

Since the unexpected discovery of low ozone values in the Antarctic in the 80s, the so-called 'Ozone Hole' has been the subject of increasing public and political interest. The term 'Ozone Hole' is used to refer to a steady lowering of about 4% in the total amount of ozone in the Earth's atmosphere. It appeared to be more significant in the northern hemisphere during springtime, particularly in the stratospheric ozone around the polar area, but scientists also noticed a decrease in the total amount of ozone worldwide. Ozone depletion occurs when large amounts of chemicals of anthropogenic origin (e.g. chlorofluorocarbons products (CFCs)), are transported from the surface to the stratosphere, where they are responsible for the breakdown of ozone molecules. Concerns about ozone depletion led to an international treaty designed to protect the ozone layers, by banning the production of CFCs, halons, and other chemical products that provoke a depletion of the ozone layer. This was agreed to in the Montreal Protocol<sup>1</sup> on the 16th of September 1987, which was the first universally ratified treaty in the history of the United Nations .

After the ozone layer's reduction was discovered, scientists heavily emphasized the consequences that this entails for the public health. The Ultraviolet Index (UVI) was created in order to communicate to the public the intensity of the UV radiation that reaches the earth's surface (McKinlay, 1987). The UVI was adopted by the World Meteorological Organization (WMO) and the World Health Organization(WHO) as a standard indicator, which is forecast by almost all meteorological services in the world. The subject became a growing concern due to the increase of UV radiation associated with the thinning of the ozone layer in the upper atmosphere and the variety of environmental and health effects, including damage of DNA structures, the increased risk of skin cancer in humans, and the impact on production of vitamin D (Čížková et al., 2018).

The UVI is an important tool for sun protection and health care, and its monitoring and forecasting is one of the main meteorological information communicated every day. In Europe, there are over 160 stations in 25 countries which measure the UV radiation and calculate the UVI (Schmalwieser et al., 2017). In Germany, the Federal Office for Radiation Protection (Bundesamt für Strahlung (BfS)) monitors the UVI at 27 meteorological stations (Figure: 1.1). One of these is located in Melpitz (51°32' N 12°56' E, see Fig. 1.1). This station started measuring the UV radiation at the end of 2018. The Melpitz station is operated by the Leibniz Institute for Tropospheric Research (TROPOS) and measures the UV radiation with a BTS2048-UV-S-WP spectroradiometer.

The erythema (skin reddening) action spectrum model describes the susceptibility of Caucasian

---

<sup>1</sup><https://theozonehole.com/montreal.htm>



Figure 1.1: The measuring stations network from the Federal Office for Radiation Protection in Germany, where Melpitz is marked with a red dot (taken from [www.bfs.de](http://www.bfs.de)).

skin to sunburn as defined by McKinlay (1987). It was adopted as an intensity to be represented by the UVI in a simple form. Because of this, the UVI is an irradiance scale computed by multiplying the erythema irradiance [ $\text{W}^*\text{m}^{-2}$ ] by a constant (Fioletov et al., 2010). The UV radiation exposure categories are shown in Figure 1.2.

Exposure Category	UV Index
LOW	0 - 2
MODERATE	3 - 5
HIGH	6 - 7
VERY HIGH	8 - 10
EXTREME	11 +

Figure 1.2: UVI color scale and international category of exhibition (Source: WHO (1995)).

The levels of UV radiation are influenced by several factors. The most influential ones are sun elevation, cloudiness, total ozone column, surface albedo, altitude and aerosol concentrations. When the sun is at a high elevation, the solar radiation passes through a shorter path of atmosphere to reach the Earth's surface. When the sun is in a lower elevation, the radiation goes through a longer path, therefore much of it is scattered and absorbed. In these instances, the radiation level that reaches the ground is lower. This factor depends on the time of the year, and the location of the chosen region of interest. At the same time, under cloudy conditions, the intensity of UV radiation is lower than under clear sky conditions. The characteristics of the place where the UVI is estimated, such as altitude and the surface albedo, also contribute to increase or reduce the radiation that reaches the earth's surface. Finally, the total ozone column (TOZ) is one of the most influential factors, since ozone absorbs most of the short UV radiation that is most harmful to humans (all UV-C radiation and part of the UV-B)

(WHO, 1995).

The main purpose of this thesis is to study the UV irradiance at the meteorological station in Melpitz, Germany under clear-sky conditions for both the simulated and observed spectral irradiance. A Radiative Transfer (RT) model set up was created using the LibRabtran software (a widely used and of free access software package for RT calculations). It allows for the computation of radiances, irradiance and actinic fluxes, and several features and assumptions possibilities can be decided by the user.

A good estimation of the UVI requires a good characterization of the atmospheric and its influence on the UV irradiance that reaches the surface. Because of this, several factors need to be taken into consideration. Some of which depend on the meteorological conditions of the location of interest (TOZ, clouds and aerosols). For this reason, the values of some of these factors were obtained from the Copernicus Atmospheric Monitoring Service (CAMS) reanalysis data set. It uses satellite retrievals for determining the most important meteorological variables, aerosols and chemical species present in the atmosphere. It is the latest global reanalysis data set of atmospheric composition produced by the European Center for Medium-Range Weather Forecasts (ECMWF) (Inness et al., 2019). The main reason for using this data set is that the ECMWF not only produce reanalysis data, they also produce a CAMS forecast data set. If the RT simulation's set up applied for this thesis show positive results, a RT modelling's set up for forecasting the UVI in Melpitz could be developed. Two sensitivity studies were done. One to determinate which of the available options are best suited for this study, and the other, to see how the simulations change when the values of some influential factors are changed, and to see if those changes agree with the literature. An other reason for this study was to compare the radiative closure between the simulations and the measurements of the UV irradiance in Melpitz and to determinate how precise the measurements are.

More detailed descriptions of the UVI and its most influential factors, the LibRadtran software and the data set used, will be presented in Chapter 2. In Chapter 3, the two sensitivity studies for the simulation inputs and different tools of the software will be tested for clear-sky conditions, in order to proceed in the definition of a proper set-up of the simulations. In Chapter 4, a description of the meteorological station in Melpitz and the instrument used for the UV radiation measurements and its out-coming product will be presented and compared with the measurements for some selected case studies. Finally, a short summary of the results will be shown in Chapter 5.

# Chapter 2

## Methods

As seen in Chapter 1, there are many factors that affect the UV radiation reaching the earth's surface. A more in depth discussion of the parameters which were analyzed in this thesis will be presented in this chapter, as will a full description of the meteorological station of Melpitz and the instrument for measuring the UV radiation. A detailed definition of the main factors for the UVI calculations and their assumptions made for this study are introduced in section 2.5.

### 2.1 Radiation

The UV radiation is a part of the electromagnetic spectrum of sunlight, with a wavelengths range between 100 and 400 nm and a part of the short-wave of the solar spectrum. The atmospheric attenuation law known as Beer-Lambert law, is an empirical relationship between the solar irradiance that reaches the Earth's surface with the total optical depth of the atmosphere and the solar zenith angle. The absorption or scattering of radiation by an optically active medium (the atmosphere), is measured by the optical depth of the medium. The solar irradiance that passes through the atmosphere, can be absorbed, scattered or transmitted by the particles present in this medium. The reduction of the intensity of a beam of radiation due to absorption and scattering is called extinction and the fraction of radiation that survives the trip over the distance ( $x$ ) is called transmittance. In the plane-parallel geometry approximation (Flat Earth approximation), the atmosphere is divided into parallel layers of infinite extensions in the  $x$ - and  $y$ -directions (Emde et al., 2016). Therefore, the properties of the atmosphere depend only on the altitude. Using this approximation, the transmittance derives from the Beer-Lambert law:

$$t(x) = \frac{I(\tau, \mu_0)}{I_0}, \quad (2.1)$$

where  $\tau$  is defined as the optical depth.  $I_0$  is the downward irradiance at the top of the atmosphere, and  $\mu_0$  is the cosine of the solar zenith angle. The incident irradiance thus decays exponentially along the slant path where the optical depth is given by  $\tau/\mu_0$ . Figure 2.1 shows an example of the transmittance (left) and the irradiance  $I$  (right) simulated for the 23 of August of 2019 at 12 UTC.

### 2.2 Measuring Station Melpitz

The meteorological station in Melpitz, Germany ( $51^{\circ}32' N$   $12^{\circ}56' E$ ) is one of the 27 active stations of the Federal Office for Radiation Protection (BfS) measuring network. It is located 86 m above sea level and is operated by the Leibniz Institute for Tropospheric Research (TROPOS). The surface UV radiation is measured with a BTS2048-UV-S-WP high-quality spectroradiometer manufactured by Gigahertz-Optik GmbH. The station site is in a field in rural Saxony, with a dominating southwesterly wind and maritime air-masses that only reach the field after crossing the majority of the western part of Central Europe. The instrument was installed at the end of 2018. Figure 2.2 shows the Melpitz station and where the BTS2048-UV-S-WP is located.

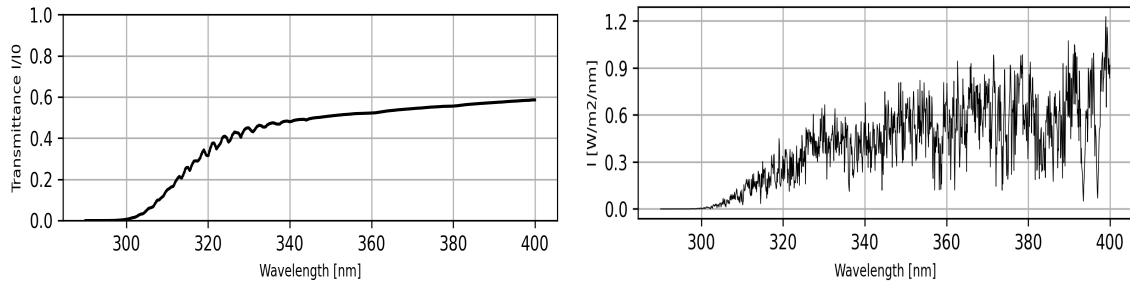


Figure 2.1: Transmittance simulated in LibRadtran for the 23/08/2019 at 12 UTC, solar zenith angle obtained from CAMS reanalysis data(right). Spectral irradiance simulated for the UV range for the 23/08/2019 at 12 UTC, solar zenith angle obtained from CAMS reanalysis data(left)



Figure 2.2: Meteorological station located in Melpitz, Germany, which is a part of the solar UV-network from the Federal Office for Radiation Protection (Source: Leibnitz-Institute for Tropospheric research).

The BTS2048-UV-S-WP is a high-quality spectroradiometer for high precision outdoor UV measurements developed and manufactured by Gigahertz-Optik GmbH (see the Gigahertz-Optik's product description for a more detailed description <sup>1</sup> ). The instrument measures solar radiation with an excellent stray-light reduction performance. Integration times from  $2 \mu\text{s}$  up to 60 s provide a high dynamic range of the instrument in the spectral range from 200 to 430 nm. This covers all the UV-A and UV-B spectrum with an optical bandwidth of 0.8 nm and a pixel resolution of  $0.13 \frac{\text{nm}}{\text{pixel}}$ . To enable stray-light-corrected measurements, a remote-controlled filter wheel with 8 positions (open, closed, optical filters) is located in the optical beam path.

One of the outstanding features of this spectroradiometer is the BiTec sensor. It combines properties of a photodiode with those of a back-thinned CCD diode array. Through bilateral correction of measurement signals from both sensors, the BiTec sensor ensures precise radiometric and spectral-radiometric measurement values over a large dynamic range. The "Solar-Scan Software" is used for the continuous scheduling of the measurement. Solar-scan exports the data in a specific ASCII-Format. With a post-processing scripts to read and visualize solar radiation data exported by the Solar-scan, the measured data is processed in order to proceed for further analysis.

## 2.3 Cams Reanalysis Data Set

The Copernicus Atmospheric Monitoring Service (CAMS) Reanalysis data set from the European Center for Medium-Range Weather Forecasts (ECMWF) was used to establish the value of some of the parameters in this study. The CAMS reanalysis data set is the latest global reanalysis data set of atmospheric compositions (AC), consisting of 3-dimensions time-consistent AC fields, including aerosols and different gases. The atmospheric composition data is available for 8 times a day (0, 3, 6, 9, 12, 15, 18, 21 UTC) and covers the period 2003-2019. The horizontal resolution is equivalent to grid spacing of approximately 80 km globally. The vertical resolution consists of 60 model levels

<sup>1</sup><https://www.gigahertz-optik.de/en-us/product/BTS2048-UV-S-WP>

with a model top at 0.1 hPa. Satellite retrievals of several variables are assimilated for the CAMS reanalysis with ECMWF's Integrated Forecast System (IFS). The IFS uses an incremental 4D-Var assimilation system, where a cost function that measures the difference between the modelling and the observations is minimized in order to obtain the best profiles possible. The atmospheric composition satellite retrievals of O<sub>3</sub>, CO, NO<sub>2</sub> and AOD are assimilated from a range of instruments and satellites (AURA, Envisat, TERRA) (Inness et al., 2019).

## 2.4 The Ultraviolet Index (UVI)

The solar ultraviolet index described by the WHO: "is a simple measure of the UV radiation level at the Earth's surface. It serves as an important vehicle to raise public awareness and to alert people about the need to adopt protective measures when exposed to UV radiation" (WHO, 1995)(p.IV).

According to several studies, the biological effects of UV radiation are highly correlated to the wavelength of the radiation. Because of this, the solar spectral irradiance  $I(\lambda)$  in  $\frac{W}{m^2*nm}$  is the main factor to be calculated, in order to prevent skin damage. The integration of the solar irradiance, in  $\frac{W}{m^2}$  or  $\frac{mW}{m^2}$ , weighted by the erythema irradiance spectrum for each wavelength, between 280 and 400 nm, multiplied by a constant  $k_{er} = 40\frac{m^2}{W}$  or  $k_{er} = \frac{1}{25}\frac{m^2}{mW}$  results in the unique and worldwide accepted ultraviolet index definition:

$$UVI = k_{er} * \int_{280}^{400} I(\lambda) * \varepsilon(\lambda) d\lambda \quad (2.2)$$

Erythema denotes the redness of the skin that is caused by solar radiation. The erythema action spectrum ( $\varepsilon(\lambda)$ ) shows the effectiveness of solar irradiance on the human skin. Therefore, this effect is defined by the spectral curve of the solar radiation with wavelengths between 280 and 400 nm that reach the earth's surface and the response of human skin to this radiation. The response of the human skin is modulated by  $\varepsilon(\lambda)$ , which was determined by McKinlay (1987) for Caucasian skin, which was decided as the standard type of skin that is contemplated in the worldwide UVI's measurements. This is something to highlight, since not all humans have the same sensitivity to UV radiation. The skin pigmentation of each person allows them to handle a certain amount of exposure to this kind of radiation. As a standard assumption, skin of type II (people with lightly pigmented white skin) is taken as a reference to establish the maximum exposure to solar UV radiation. This coefficient allows to estimate the minimum required exposure to solar radiation, so that no biological damage happens:

$$\varepsilon(\lambda) = \begin{cases} 1 & \text{for } 280 \leq \lambda \leq 298 \text{ nm} \\ 10^{[0.094(298-\lambda)]} & \text{for } 299 \leq \lambda \leq 328 \text{ nm} \\ 10^{[0.015(339-\lambda)]} & \text{for } 329 \leq \lambda \leq 400 \text{ nm} \end{cases} \quad (2.3)$$

In Figure 2.3, the sunburning action spectrum defined by equation 2.3 is shown in the red curve. Vitamine D is needed by humans for several biological processes and its action spectrum is shown by the green curve. As can be seen in both curves, the action spectrums show maximums in the UV-B range, while they decrease rapidly in the UV-A range. From the solar irradiance that reaches the surface (blue curve), about 94 % of the energy corresponds to UV-A, while only 6 % belongs to UV-B. However, as demonstrated by the red curve, when the wavelength is larger than 320 nm, the changes in solar irradiance do not greatly affect the UVI, while changes in the UV-B range (295-315 nm) produce significant changes to the erythema irradiance. On the other hand, the purple curve shows the coefficient for the ozone absorption, which occurs mostly in the stratosphere and is the main responsible for decreasing the UV radiation in the atmosphere.

## 2.5 Important Factors Influencing the UVI

The amount of UV radiation that reaches the surface is influenced by significant number of astronomical and meteorological parameters. Accordingly to WHO (1995) and a sensitivity study by Allaart et al. (2004), the parameters and variables that introduce the highest degree of uncertainty in the

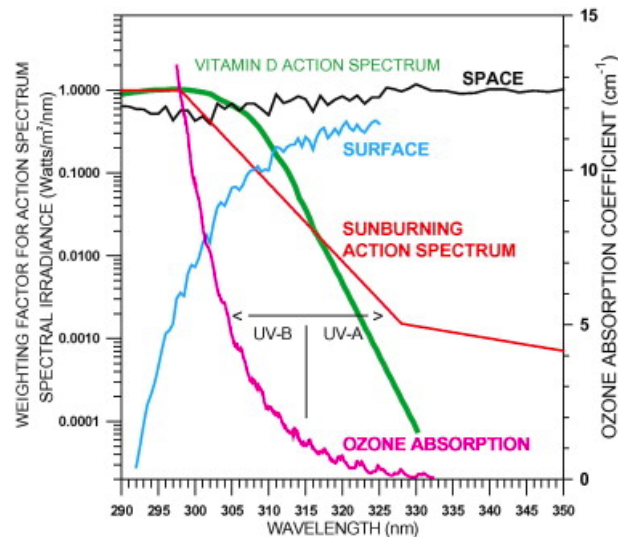


Figure 2.3: Representation of the global irradiance that reach the surface on a summer day (blue curve), erythema action spectrum (red curve), vitamin D action spectrum (green curve) and ozone absorption (purple curve) (Fioletov et al., 2009).

variability of the UVI are the solar zenith angle, the total ozone column, cloud cover, surface albedo, aerosols, and altitude, further details of each will be presented later in this section, as will, some of the assumptions that were made for the set-up of the simulations.

### 2.5.1 Solar Zenith Angle (SZA)

The Solar Zenith Angle (SZA) is defined as the angle between the solar and the zenith direction and has a range between  $0^\circ$  and  $90^\circ$ . The solar zenith angle affects both the optical path through the atmosphere and the angular distribution of solar radiation. The higher the elevation of the sun, the lower the SZA and the higher the UV radiation. As the SZA increases, the radiation has to go through a thicker atmosphere and more radiation is absorbed and scattered by the particles present. In those cases, the effect of ozone and aerosols become more important. A reduction of about 17 % was estimated by Badosa (2002) in the UVI, when the SZA varies from 0 to 60 degrees. The SZA can be easily calculated when the time of the year, latitude and longitude of the location are known.

In the first analysis (Chapter 3), two SZAs of 30 and 60 degrees, were used. Throughout the rest of this thesis, the SZA will be taken from the CAMS data.

### 2.5.2 Total Ozone Column (TOZ)

The Total Ozone Column (TOZ) is one of the most important factors that should be considered when UVI is calculated, since it is responsible for the absorption of all UV-C and much of the UV-B radiation. TOZ is defined as the thickness that the column of ozone would have if it had a standard temperature and pressure ( $0^\circ\text{C}$  and 1 atm). The TOZ is generally presented in Dobson Units (DU), where 1 DU of ozone corresponds to  $2.69 \times 10^{20}$  molecules per  $\text{m}^2$  in an ozone column. However, the influence of the vertical distribution of ozone on UVI is less important than that of TOZ. It was calculated through modelling simulations, that the UVI was increased by up to 8 % (for SZA conditions from  $0^\circ$  to  $80^\circ$ ) when a mid-latitude ozone profile was replaced by a tropical profile, which is an extreme scenario (Allaart et al., 2004).

The total ozone column in Dobson Units (DU) was analyzed using the CAMS reanalysis data that were available. The mean TOZ time series and their yearly statistical distribution are presented in Figure 2.4. Here can be seen, not only the yearly statistic distribution for the whole period (on the left), but also the mean distribution (plot on the right) in blue, and the mean with and without the standard deviation (green and orange curves respectively). Each of the yearly distributions can be found in Appendix A. In this case, a seasonal distribution of the total amounts of ozone can be clearly

observed. The seasonal variability does not change significantly year to year. For these reasons and since the purpose of the following chapter is to show how this variable affects the UVI simulation, a fixed values was determined. This value is TOZ=335 DU, which is the mean values calculated for the whole period.

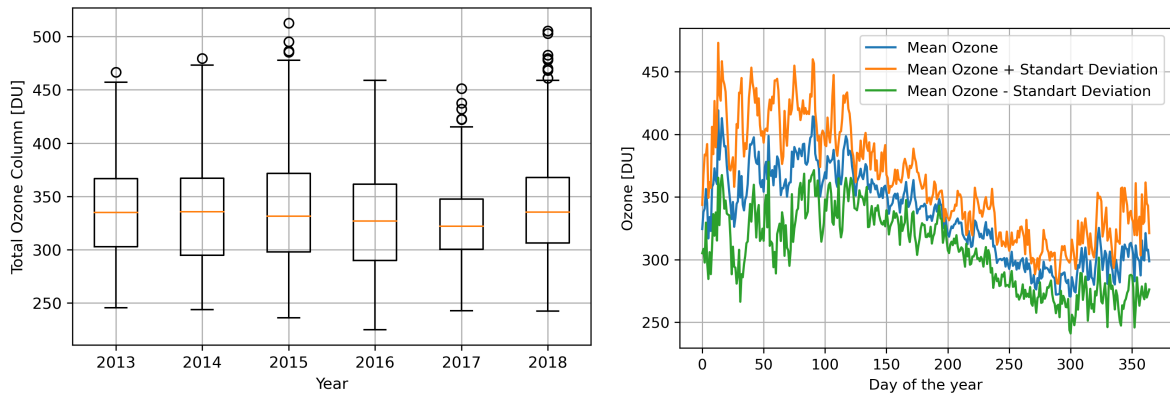


Figure 2.4: Total Ozone Column statistical distribution (left) and time series distribution of the mean TOZ in the period 2013-2018 (right). Produced via CAMS Reanalysis for Melpitz.

### 2.5.3 Clouds

Cloud cover generally reduces UV radiation levels but sometimes the scattering produced in the presence of some degree of cloud cover can have the same effect as the reflectance by different surfaces, producing an increment in the total UV radiation levels. There are many available studies of the effect of clouds on the UVI. For example, Sabburg and Wong (2000) found that 3% of the cases of UV-B measurements, showed enhancements up to 8% due to the presence of cirrus clouds or turbidity. Renaud et al. (2000) showed a decrease in UVI of about 8% for thick clouds and 70% for thin clouds in overcast conditions.

The temporal and spatial variability of clouds and their characteristics are so complex, that many forecasts issue "clear-sky" UVI forecasts instead of eliminating this source of error. The amount and properties of clouds can produce an uncertainty up to 50% on the estimation of the UVI. However, since the complexity due to the strong temporal and spatial variability of this is so high, this parameter will not be taken in consideration for this thesis. If this parameter was to be taken into consideration, the UVI is usually calculated for clear sky conditions and a correction is made afterwards, depending on the properties of the clouds.

### 2.5.4 Surface Albedo

The surface albedo is the percentage of the radiation that is reflected by an horizontal surface, which depends on the wavelength and the characteristics of the ground. Most of the surfaces have an UV albedo between 2-5%, but when the ground is covered by snow, the UV albedo can have a value up to 0.8. A UV-B increase of 28% over snow cover and under clear sky conditions has been reported by McKenzie et al. (1998); Chadyšiene and Girgždys (2008). The ultraviolet albedo is quite low for most surfaces, and so the influence on the UVI is minimal. However, in the presence of snow or sand, it can produce an increase on the UVI since most of the radiation is reflected by the ground.

In the next chapter, a sensitivity study of how the most influential variables affect the RT simulations will be presented. In that study, a value of 0.2 for all the wavelengths will be taken as a reference case, while other values for this factor will be tested.

### 2.5.5 Aerosol Optical Depth (AOD)

The presence of aerosols in the atmosphere, scatters and absorbs the solar radiation, generating an increase of the diffuse component of the solar radiation and a decrease of the direct component.

The global (direct + diffuse) irradiance is usually lower than when the aerosols are not taken in consideration. To explain the aerosol properties for the radiative transfer calculations the following three variables have to be known at each wavelength: aerosol optical depth (AOD), Aerosol Single-Scattering Albedo (SSA), and phase function, which is usually simplified through the asymmetry factor ( $g$ ).

The AOD is a measure of the extinction of the solar beam by the particles in the atmosphere (dust, smoke, pollution, etc.). The AOD tells us how much direct sunlight is prevented from reaching the ground by these aerosol particles. Several studies have analyzed the importance of this factor and how it can affect the UVI calculations.

The SSA is defined as the ratio of the scattering to the extinction. Extinction is the sum of scattering and absorption. When photons are scattered, the wavelength remains unchanged. SSA is a function of wavelength.

Once again, using the CAMS reanalysis data available, the values of Aerosol Optical Depth (AOD) were determined. The CAMS reanalysis data does not estimate the AOD in the range of ultraviolet radiation. Therefore, the two shortest wavelengths were used. These were the  $AOD_{469}$  and  $AOD_{865}$ . Figure 2.5 shows the statistics for the yearly distributions of both  $AOD_{469}$  (on the left) and  $AOD_{865}$  (on the right), for the closest grid point to Melpitz ( $51^{\circ}N 12^{\circ}75'E$ ).

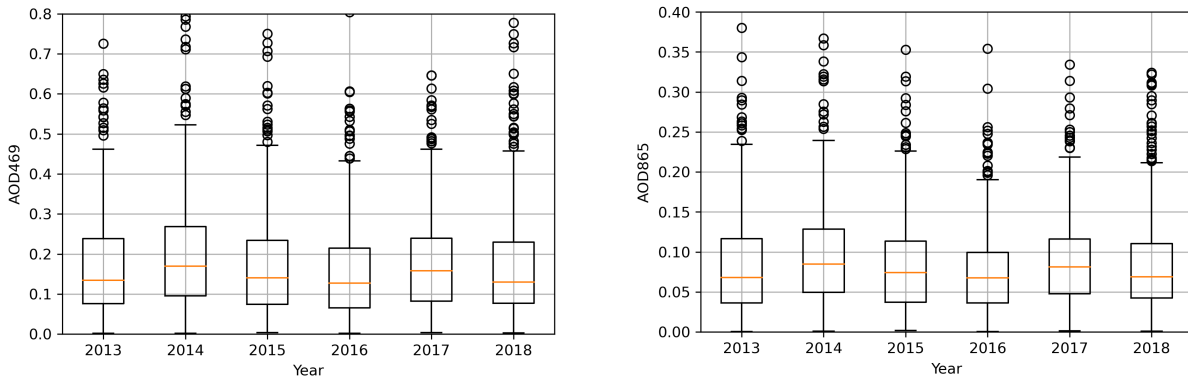


Figure 2.5: Statistical distribution for aerosol optical depth at 469 nm (left) and 865 nm (right); plotted from CAMS Reanalysis for Melpitz.

As it can be seen in the plot, the mean values do not change significantly from year to year, but it can also be seen that there are several episodes of high aerosols concentrations. This means that there is a high number of particles in the atmosphere, that extinguished a higher amount of direct solar radiation, and therefore, less direct radiation reaches the surface. On the other hand, it increases the intensity of the diffuse radiation that reaches the ground. For this reason, it has been decided to use the mean values for this first sensitivity test. The calculated mean values are 0.1795 and 0.0884 for the  $AOD(469\text{ nm})$  and  $AOD(865\text{ nm})$  respectively (see the rest of the graphics in the Appendix A). Once the values for both the AODs were established, the Ångström coefficients (Ångström, 1961) were calculated, with the following equation:

$$AOD(\lambda) = \beta * \lambda^{-\alpha} \quad (2.4)$$

where  $\beta$  is the optical thickness at  $1\text{ }\mu\text{m}$  and  $\alpha$  explains the change of AOD with the wavelength.  $\beta$  represents the number of aerosols in the atmosphere and  $\alpha$  has to do with the size of the aerosols particles. This means, the larger the  $\alpha$ , the smaller the particles, with a maximum value of 4, corresponding to a strong Rayleigh scattering. After resolving equation 2.4, the values of 1.154 and 0.075 for  $\alpha$  and  $\beta$ , respectively, were set as input for the modelling.

### 2.5.6 Altitude

As altitude increases, a portion of atmosphere is left underneath, this reduces radiation extinction and, thus, causes an increase in UVI. The altitude of the location where the UVI is calculated, can produce

an increase of the UVI of 10 to 12% for every 1000 m. This effect is associated with a decrease in the Rayleigh scattering, under clear-sky conditions and low presence of aerosols (WHO, 1995). Above sea level, ground surfaces are often mountainous, sometimes being semi-snow covered, and the atmosphere always contains some pollution that varies vertically, horizontally, and temporally. Because of this, the observed altitude effect varies greatly from place to place. Since the meteorological station of Melpitz is at an altitude close to sea level, this variable will not be taken in consideration for the further analysis into this thesis.

## 2.6 Radiative Transfer Model

There are several available RT simulation softwares for analyzing the UV radiation, but in this thesis, the LibRadtran software was selected. The LibRadtran software package is a library of radiative transfer programs and routines for solar and thermal radiation in the earth's atmosphere, which is a useful software for RT calculation. RT modelling is used for many different calculations in several fields of study, and a key subject for remote sensing the planetary atmosphere. This software includes several tools for simulating most of the factors which affect the atmosphere's radiation. It includes different equations solvers which can be chosen for modelling the needed parameters (Mayer and Kylling, 2005; Emde et al., 2016). It can be used for many applications, some of the most common are the calculation of radiance, irradiance, remote sensing of clouds and aerosols, or UV forecasting. The latest description can be found on the LibRadtran website<sup>2</sup> or in the latest publication<sup>3</sup>. The software is free access and is continuously being improved and developed for new features by the users and the LibRadtran developers.

The central program of the package is an executable called *UVSPEC*, a calculation of the spectral irradiance and actinic flux in the ultraviolet and visible ranges of the solar spectrum. The original code was developed by Kylling (1993). Nowadays, the *UVSPEC* routine includes the full solar thermal spectrum from 100 nm to 120  $\mu\text{m}$ . An input file with all the parameters and assumptions is required to run the simulations. It must contain the parameters describing which type of atmosphere should be used and several set-up options, like which the 10 different radiative transfer equation resolvers should be used for initializing the software. Figure 2.6 shows the overall structure of the *uvspec* model.

In Figure 2.6, the order and steps for the configuration of the model's input file and process to be performed by the software are presented. At first, the atmospheric state needs to be provided by the user as an input file. If the user does not provide an atmospheric file, a US-standard atmospheric file will be selected from the software. Secondly, the user decides which of the various parametrizations for converting the atmospheric state into optical properties is used. Then the optical properties are passed through one of the radiative transfer equation (RTE) solvers, according to the processing time and precision required by the user. Finally, the user can choose which variable, units and processes from amongst the options available for each RTE resolver.

For the RT simulations of the irradiance in Melpitz, some features of the LibRadtran software were established for a proper model set-up. These features needed to be defined for the model to work properly and for the simulations to calculate the desire outputs.

The RTE solver chosen for this purpose, was the DIScrete ORdinate Radiative Transfer solver (DISORT) (Stamnes et al., 2000). As its name suggest, it is based on discrete ordinates and allows accurate calculations of irradiance, radiances and actinic fluxes in a 1-Dimention plane-parallel geometry. This is a fast and precise solver and was last updated in 2011 by Buras et al. (2011).

Secondly, the solar resolution of 0.1 nm was established, to obtain the results within the highest extraterrestrial spectrum resolution available and for a good comparison with the observations.

Then the number of streams used to solve the radiative transfer equation were chosen, to analyze if there are significant differences to be considered when the number of streams is low. The number of streams is the numbers of quadrature angles that the software uses for solving the solar equations. This is important for the computational processing, because the higher the number of streams, the slower

---

<sup>2</sup><http://www.libradtran.org>

<sup>3</sup>libRadtran/doc/libRadtran.pdf

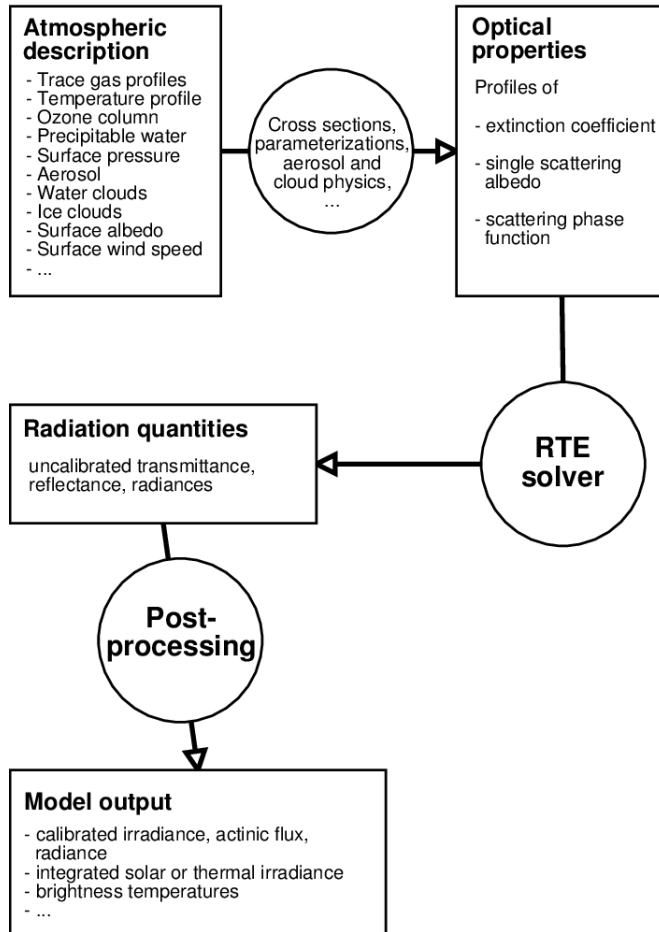


Figure 2.6: Structure of the *uvspec* radiative transfer model (Emde et al., 2016).

and the more precise the simulations should be. Therefore, for the first sensitivity study, (presented in Chapter 3), three numbers of streams were chosen ( $N= 4$ ,  $N=8$  and  $N=16$ ).

At least, 3 molecular absorption parametrizations (MAPs) were used for the first simulations. The first one was the REPTRAN parametrization (Gasteiger et al., 2014), which integrates over a narrow spectral bands with a spectral resolution of  $15\text{ cm}^{-1}$ . It is Libradtran's default setting in case it is not defined by the user. Secondly, the CRS model was tested. This switches off spectral parametrizations and only molecular absorption cross sections are considered. The last one to be tested, was the LOWTRAN (low-resolution transmission) parametrization. This performs Pseudo-spectral calculations with exponential-sum-fit, with a  $20\text{ cm}^{-1}$  resolution.

# Chapter 3

## Sensitivity Studies

In this chapter two sensitivity studies will be presented. This were done to determinate some of the model's input configuration as well as to show how some of the main parameters affect the RT simulations of UV irradiance.

During the first sensitivity study three different molecular absorpcion parametrizations, three options for the number of streams and two SZAs were analyzed. Some inputs were used as mentioned in chapter 2 (TOZ, aerosols and albedo). While other inputs were decided after studying the available literature (Stamnes et al., 2000; Mayer and Kylling, 2005; Emde et al., 2016). Those were the RTE solver DISORT (Van Weele et al., 2000) and the standard atmopheric file (US-Standard created by Anderson et al. (1986)).

After some model inputs were analyzed, a second sensitivity study to determine and to show how some of the parameters mentioned in the previous chapters impact on the simulation using the set-up model and if this results fits with previous studies in this subject (Badosa and Weele, 2002; Fioletov et al., 2009; Alfaro Lozano et al., 2016). The values obtained in the previous sensitivity study were used as references for this part of the study. The variables to be analyzed in Section 3.2 are the surface albedo, TOZ and AOD.

### 3.1 LibRadtran Model Configuration's Inputs Sensitivity Study

In this section, the main input settings for the simulations set up will be studied.

For this part of the study, some factors were set as a standard configuration, such as albedo (0.2), the 19/06 (day of the year=170), and a the default atmosphreic file (US-standard) used by LibRadtran. The chosen day corresponds to a summer day and, therefore, no snow conditions will be taken into consideration. The determination of a specific date, helps the model to correct the calculated radiation quantities for the Sun-Earth distance for a specific Julian day. Since the purpose of this study is to analyze UV radiation in the ultraviolet spectrum, the wavelength range was defined as 280-400 nm, with a resolution of 0.1 nm, for the simulations.

Three molecular absorption parametrizations, two different solar zenith angles of 30° and 60° and three different options for the number of streams ( $n=4$ ,  $n=8$  and  $n=16$ ) were used for this sensitivity study. The two SZAs were chosen to show how important this variable is for the UVI calculations and to be able to estimate how the calculations of the different component of the solar radiation (direct, diffuse and global radiation) differ in each case. At the same time, three options for the number of streams were used in each instance, to analyze if there was a significant difference in the precision of the modelling and its time of processing. Table 3.1 presents all the parameters used for the set up of the simulations during the first sensitivity study.

### Results

Table 3.2 shows the results of the different simulations. It shows the UVI estimated using the global irradiance presented through the Equation 2.3 for each case. The estimated UVI when SZA=30° were between 7.94 (REPTRAN) and 8.11 (LOWTRAN), while for SZA=60° were between 1.87 (REP-

Table 3.1: Set-up parameters and assumptions for model configuration's inputs sensitivity study.

SZA	30° / 60°
TOZ	335 DU
Albedo	0.2
Angstrom Coefficients	$\alpha = 1.154$ and $\beta = 0.0748$
AOD(550 nm)	0.1495
RTE solver	DISORT
UV (280-400 nm) Resolution	0.1 nm
Molecular Absorption Parametrization	REPTRAN / CRS / LOWTRAN
Number of Streams	4 / 8 / 16

TRAN) and 1.92 (LOWTRAN). The absolute different of the UVIs seem larger when the SZA is closer to the zenith. This is related to the fact that a stronger amount of solar irradiance reaches the surface when the sun is at a higher elevation. Another observation is that increasing the amount of streams, requires a larger computational processing time (approx. 6 seconds for LOWTRAN and approx. 10 seconds for REPTRAN), and it produces a difference of less than 1 W per  $m^2$  in the global irradiance obtained for each molecular absorption parametrization. This small difference implies a difference of less than 1% in the calculated UVI. On the other hand, the differences using the different molecular absorption parametrizations represent a discrepancy of almost 2 W per  $m^2$  in the global irradiances and each of its components, and less than 0.2 in the UVIs calculations. The main differences can be seen in the UV-A range, which does not produce a strong difference in the UVI. All the plots for the simulated irradiances and their weighted curves with the erythema action spectrum are attached in Appendix A.

On the basis of these results, it was decided to use the molecular absorption parametrization REPTRAN with 16 streams. Knowing that it requires the largest processing time, but is also the latest improved parametrization, makes it the most precise of all the ones tested (Gasteiger et al., 2014). During this study only a selected number of cases were simulated, for that reason, it was decided to use the most time-consuming and precisest molecular absorption parametrization.

## 3.2 Meteorological Inputs Sensitivity study

In this section, a more detailed sensitivity study will be introduced for the most influential factors TOZ, surface albedo and aerosols present in the atmosphere, in order to determine how these parameters affect the RT simulations and to corroborate the results with the studied literature. The three studies were done separately, to determine the effects of each of these parameters separately.

### 3.2.1 Total Column Ozone

The TOZ is one of the most important parameters that must be considered for UVI calculations. As shown by Allaart et al. (2004), this variable introduces an uncertainty of about 4 % in the calculations of the UVI. For this reason, four scenarios where only the TOZ value was changed, were simulated and the UVI was calculated. The reference case is the annual mean value for the 2013-2018 period (TOZ=335 DU calculated from CAMS reanalysis). The parameters used for the set up used in this section are shown in Table 3.3. The values chosen for this sensitivity study represent typical seasonal values of TOZ for Melpitz, which are illustrated in Figure 2.4. The seasonal variability of the total amount of ozone is strong in mid-latitudes. For Melpitz the values above the 335 DU usually correspond to the first half of the year, while the ones below, are usual for the second part of the year.

## Results

The result of the simulation are shown in Figure 3.1, where the erythema weighted solar irradiance and the erythema action spectrum are illustrated. The main differences between the simulations are in the range of the UV-B irradiance (290 and 315 nm). This agrees accordingly with the theory that

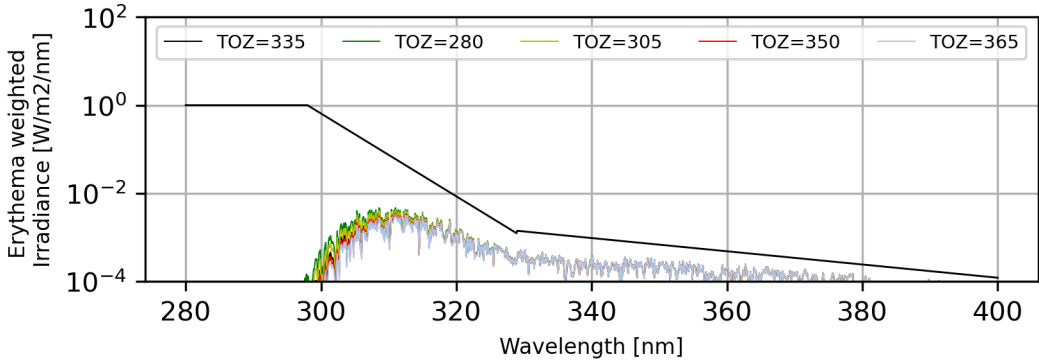
Table 3.2: Results obtained for model configuration's inputs sensitivity study.

Streams	REPTRAN			CRS			LOWTRAN			
	SZA	UV-B [ $\frac{W}{m^2}$ ]	UV-A [ $\frac{W}{m^2}$ ]	UVI	UV-B [ $\frac{W}{m^2}$ ]	UV-A [ $\frac{W}{m^2}$ ]	UVI	UV-B [ $\frac{W}{m^2}$ ]	UV-A [ $\frac{W}{m^2}$ ]	UVI
4	30°	$F_{dir} = 0.56$	$F_{dir} = 27.52$		$F_{dir} = 0.56$	$F_{dir} = 27.52$		$F_{dir} = 0.56$	$F_{dir} = 27.61$	
		$F_{dif} = 0.96$	$F_{dif} = 25.83$	7.94	$F_{dif} = 0.96$	$F_{dif} = 25.83$	7.95	$F_{dif} = 0.97$	$F_{dif} = 25.92$	8.11
		$F_{glob} = 1.52$	$F_{glob} = 53.36$		$F_{glob} = 1.52$	$F_{glob} = 53.36$		$F_{glob} = 1.54$	$F_{glob} = 53.53$	
4	60°	$F_{dir} = 0.05$	$F_{dir} = 8.14$		$F_{dir} = 0.05$	$F_{dir} = 8.14$		$F_{dir} = 0.05$	$F_{dir} = 8.19$	
		$F_{dif} = 0.29$	$F_{dif} = 16.69$	1.87	$F_{dif} = 0.29$	$F_{dif} = 16.69$	1.88	$F_{dif} = 0.3$	$F_{dif} = 16.79$	1.91
		$F_{glob} = 0.34$	$F_{glob} = 24.84$		$F_{glob} = 0.35$	$F_{glob} = 24.84$		$F_{glob} = 0.35$	$F_{glob} = 24.98$	
8	30°	$F_{dir} = 0.56$	$F_{dir} = 27.52$		$F_{dir} = 0.56$	$F_{dir} = 27.52$		$F_{dir} = 0.56$	$F_{dir} = 27.61$	
		$F_{dif} = 0.96$	$F_{dif} = 25.85$	7.95	$F_{dif} = 0.96$	$F_{dif} = 25.86$	7.97	$F_{dif} = 0.97$	$F_{dif} = 25.94$	8.13
		$F_{glob} = 1.52$	$F_{glob} = 53.38$		$F_{glob} = 1.52$	$F_{glob} = 53.38$		$F_{glob} = 1.54$	$F_{glob} = 53.55$	
8	60°	$F_{dir} = 0.05$	$F_{dir} = 8.14$		$F_{dir} = 0.05$	$F_{dir} = 8.14$		$F_{dir} = 0.05$	$F_{dir} = 8.19$	
		$F_{dif} = 0.29$	$F_{dif} = 16.78$	1.88	$F_{dif} = 0.29$	$F_{dif} = 16.78$	1.89	$F_{dif} = 0.3$	$F_{dif} = 16.87$	1.92
		$F_{glob} = 0.35$	$F_{glob} = 24.92$		$F_{glob} = 0.35$	$F_{glob} = 24.95$		$F_{glob} = 0.35$	$F_{glob} = 25.06$	
16	30°	$F_{dir} = 0.56$	$F_{dir} = 27.52$		$F_{dir} = 0.56$	$F_{dir} = 27.52$		$F_{dir} = 0.56$	$F_{dir} = 27.61$	
		$F_{dif} = 0.96$	$F_{dif} = 25.85$	7.95	$F_{dif} = 0.96$	$F_{dif} = 25.85$	7.97	$F_{dif} = 0.97$	$F_{dif} = 25.94$	8.13
		$F_{glob} = 1.52$	$F_{glob} = 53.38$		$F_{glob} = 1.52$	$F_{glob} = 53.38$		$F_{glob} = 1.54$	$F_{glob} = 53.55$	
16	60°	$F_{dir} = 0.05$	$F_{dir} = 8.14$		$F_{dir} = 0.05$	$F_{dir} = 8.14$		$F_{dir} = 0.05$	$F_{dir} = 8.19$	
		$F_{dif} = 0.29$	$F_{dif} = 16.77$	1.88	$F_{dif} = 0.29$	$F_{dif} = 16.77$	1.89	$F_{dif} = 0.3$	$F_{dif} = 16.77$	1.92
		$F_{glob} = 0.35$	$F_{glob} = 24.92$		$F_{glob} = 0.35$	$F_{glob} = 24.92$		$F_{glob} = 0.35$	$F_{glob} = 25.06$	

Table 3.3: Set-up parameters and assumptions for analyzing the effects of TOZ in the RT simulations.

UV (280-400 nm) Resolution	0.1 nm
RTE Solver	DISORT
Molecular Absorption Parametrization	REPTRAN
SZA	60°
Ångström Coefficients	$\alpha = 1.154$ and $\beta = 0.0748$
Albedo	0.2
TOZ	280/305/335/350/365

the ozone absorption spectrum presents its maximum at approximately 295 nm and decreases rapidly when the wavelength increases (WHO, 1995; Badosa, 2002; Fioletov et al., 2009).

Figure 3.1: Erythema weighted irradiances for sensitivity study for the effects of TOZ on the RT simulations using *UVSPEC* model in the UV spectrum.

The results obtained from these simulations are represented in Table 3.4. Here the UVI is calculated for the total UV range and for the UV-A and UV-B ranges, to demonstrate how this parameter affects the estimation of the solar irradiance in each of the ranges. At the same time this shows the importance of the weighted irradiance with the erythema spectrum in the range of UV-B. In this case, a difference of less than  $1 \frac{W}{m^2}$  in the range of 280-315 nm produces a difference of 0.4 in the calculated UVI. This results corroborate the literature already mentioned and shows how important a good definition of this factor is for the UVI estimation. At the same time, if there would be a low ozone scenario like when the ozone hole was discovered, the irradiance that would reach the surface could be quite high, and that situation could be dangerous for humans.

Table 3.4: Results of RT simulations to determine the effects of TOZ on the UV irradiance simulations.

TOZ [DU]/ Difference [%]	UVI Range (280-315) [-]/ UV-B Radiation [W/m²]	UVI Range (315-400) [-]/ UV-A Radiation [W/m²]	Global Irradiance [W/m²]	UVI [-]	Effect on UVI [%]
335	0.93 / 0.35	0.95 / 24.93	25.27	1.88	
280 / 19.64	1.33 / 0.45	0.99 / 25.06	25.51	2.32	+0.44 (23.45%)
305 / 9.83	1.12 / 0.40	0.97 / 24.99	25.40	2.10	+0.21 (11.54%)
350 / 4.28	0.85 / 0.32	0.94 / 24.89	25.21	1.79	-0.09 (4.89%)
365 / 8.95	0.78 / 0.3	0.92 / 24.85	25.16	1.71	-0.17 (9.28%)

### 3.2.2 Surface Albedo

The Earth's reflection dose is characterized by the surface albedo and which is one of the parameters that has to be taken into account for the UVI calculations. The surface albedo is the fraction of radiation that is reflected by the ground. The larger the surface albedo, the more radiation is reflected by the surface. In that case, the reflected radiation adds to the global radiation, producing an increase on the UVI. For this reason, the UVI calculations should consider this parameter. This factor depends

on the surfaces characteristics. The location and time of the year are important for places where snow conditions are possible. A surface covered by snow can produce an albedo up to 1. Therefore, the uncertainty in UVI calculations that can be produced by the surface albedo is up to 28% under clear sky and fresh snow conditions (Allaart et al., 2004; Alfaro Lozano et al., 2016).

Since a summers day was chosen for this sensitivity study, and to analyze the RT simulations for Melpitz, small values (no snow) were set for the surface albedo. Taking into consideration the first sensitivity study presented in the previous section, a reference case of surface albedo=0.2 was chosen for this second sensitivity study. LibRadtran uses a single value for the entire wavelength range, unless a file where the albedo for each wavelength is defined. The assumptions used for the sensitivity study of this section are presented in Table 3.5 and the results are described in the following subsection.

Table 3.5: Set-up parameters and assumptions for analyzing the effects of surface albedo in the RT simulations.

UV (280-400 nm) Resolution	0.1 nm
RTE Solver	DISORT
Molecular Absorption Parametrization	REPTRAN
SZA	60°
Ångström Coefficients	$\alpha = 1.154$ and $\beta = 0.0748$
TOZ	335
Albedo	0/0.1/0.2/0.3/0.4

## Results

The results of the simulations are shown in Figure 3.2. It can be seen that there does not appear to be significant differences between the weighted irradiances. The main difference to see, is that the irradiance curve is displaced to higher values in the y-direction when the surface albedo is higher. For low values of surface albedo, the global irradiance in the UV range is lower than the reference case, and therefore, the estimated UVI is smaller. The results of these RT simulations are shown in Table 3.8, where the results are shown for each of the UV's wavelength ranges. In this case, the variation of the surface albedo does not just affect the UV-B irradiance, as was the case with the TOZ. The irradiances in the whole UV spectrum present differences when this parameter varies. When the surface albedo is set to double (as in the reference case), an absolute variation of less than 0.2 on the UVI is observed. The influence of this parameter should be analyzed under snow conditions, in order to determine how it might affect the RT simulations.

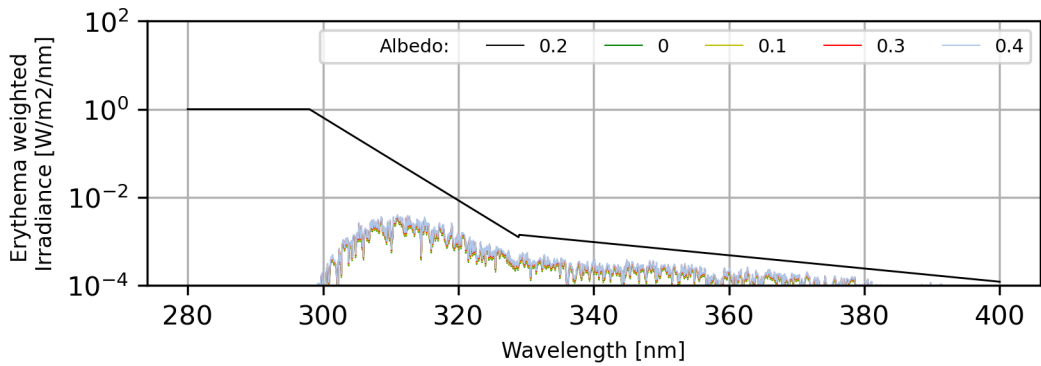


Figure 3.2: Erythema weighted irradiances for sensitivity study for the impact of surface albedo on the RT simulations using *UVSPEC* model in the UV spectrum.

### 3.2.3 Aerosol Optical Depth

The last factor that has been included for this sensitivity study, was aerosols. For this, the AOD(550 nm) was calculated from the CAMS reanalysis in the period 2013-2018. These parameter was studied,

Table 3.6: Results of RT simulations to determine the effects of surface albedo on the UV irradiance simulations.

Surface Albedo	UVI Range (280-315) [-]/ UV-B Radiation [W/m <sup>2</sup> ]	UVI Range (315-400) [-]/ UV-A Radiation [W/m <sup>2</sup> ]	Global Irradiance [W/m <sup>2</sup> ]	UVI [-]	Effect on UVI [%]
0.2	0.93 / 0.35	0.95 / 24.93	25.27	1.88	
0	0.86 / 0.32	0.87 / 23.29	23.61	1.74	-0.14 (7.68 %)
0.1	0.89 / 0.33	0.91 / 24.07	24.41	1.81	-0.07 (4 %)
0.3	0.97 / 0.36	0.99 / 25.83	26.20	1.96	+0.08 (4.35 %)
0.4	1.01 / 0.38	1.03 / 26.81	27.19	2.05	+0.17 (9.09 %)

in order to show how the aerosol affect the RT simulations. Using Equation 2.4, the AOD(550 nm) was inferred using the two available AODs mean values, assuming the same atmospheric conditions. This calculation is useful when the AOD values is determined with one instrument and must be compared to values from another instrument that uses different wavelengths or just to compare with a standard and well known AOD( $\lambda$ ).

In this case, the inferred AOD(550 nm)=0.1495 was set as the reference case. Values between 0 (no aerosols present in the atmosphere) and 0.4 (a quite hazy atmosphere) were used for the simulations set ups. A more detailed description of the inputs used for this sensitivity study are presented in table 3.7.

Table 3.7: Set-up parameters and assumptions for analyzing the effects of aerosols in the RT simulations.

UV (280-400 nm) Resolution	0.1 nm
RTE Solver	DISORT
Molecular Absorption Parametrization	REPTRAN
SZA	60°
Albedo	0.2
TOZ	335
AOD(550 nm)	0.1495/0/0.05/0.2/0.4

## Results

The results of the simulations and the UVI calculations are presented in Table 3.8. The characteristics of the aerosol particles present in the atmosphere were simulated from the mean AODs calculated for the period 2013-2018 from the CAMS reanalysis data set. An analysis of the effect of aerosols, gives an idea of how much of the UV radiation is extinguished by the atmosphere before it reaches the surface.

Table 3.8: Results of RT simulations to determine the effects of aerosols on the UV irradiance simulations.

AOD(550 nm) [-]	UVI Range (280-315) [-]/ UV-B Radiation [W/m <sup>2</sup> ]	UVI Range (315-400) [-]/ UV-A Radiation [W/m <sup>2</sup> ]	Global Irradiance [W/m <sup>2</sup> ]	UVI [-]	Effect on UVI [%]
0.1495	0.93 / 0.35	0.95 / 24.93	25.28	1.88	
0	1.01 / 0.38	1.03 / 26.93	27.32	2.04	0.16 (8.6%)
0.05	0.98 / 0.37	1.00 / 26.27	26.64	1.99	0.10 (5.75%)
0.2	0.90 / 0.34	0.92 / 24.27	24.61	1.83	-0.05 (-2.78%)
0.4	0.81 / 0.3	0.83 / 21.94	22.24	1.64	-0.24 (-12.75%)

As was expected, when a larger number of particles are present in the atmosphere, less solar radiation reaches the surface and, therefore, the UVI values are smaller. In this case, the extinction of UV radiation is stronger, since there is a larger concentration of aerosols in the atmosphere. At the same time, it should be noted, that when there is a hazy atmosphere, the total UVI does not vary as

strong as with changes in other parameters (TOZ and SZA). Also, the presence of aerosols affects the irradiance for the whole UV range of the spectrum. The results of the RT simulations are illustrated in Figure 3.2. A further analysis for Melpitz of the influence of the different properties of aerosols could be performed in another study as the one published by Badosa and Weele (2002). A further sensitivity study of the effects that aerosol produce on UVI estimations should be performed for more SZAs. It should be expected that the effect of aerosols is lower when the sun is at a higher elevation.

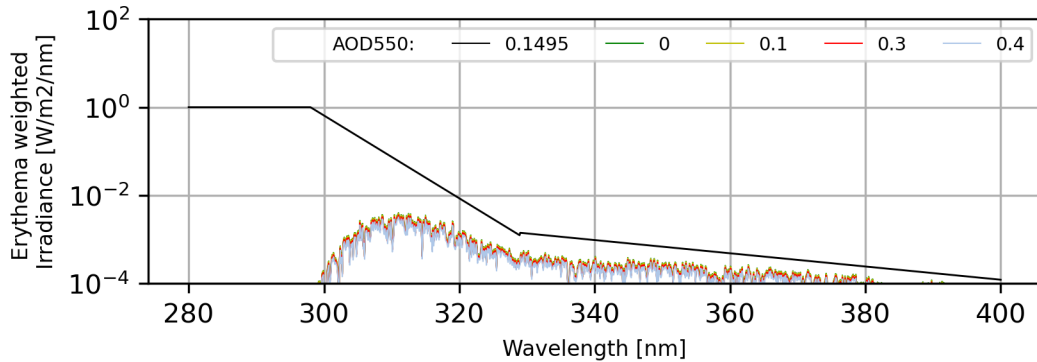


Figure 3.3: Erythema weighted irradiances for sensitivity study for the effects of aerosols on the RT simulations using *UVSPEC* model in the UV spectrum.

# Chapter 4

# Comparison of RT Simulations and Observations

In this chapter, the simulations that have been introduced and tested in the previous chapters, will be compare with the measurements which have been running in Melpitz, Germany ( $51^{\circ}32' N$   $12^{\circ}56' E$ , 86 m above sea level) since the end of 2018. This is a new station of the German Federal Office for Radiation Protection measuring network for monitoring solar ultraviolet irradiance. It is operated by the Leibniz Institute for Tropospheric Research (TROPOS) using a high-quality spectroradiometer for high precision outdoor UV measurements.

## 4.1 Cases Studies

In this section, the RT simulations will be compared with measurements from a BTS2048-UV-S-WP spectroradiometer for a selected number of cases from the year 2019. The selected cases were analyzed with satellite images (not shown) using the SEVIRI satellite instrument, to see if those days had mostly clear-sky conditions. After analyzing the cases where mostly clear-sky conditions were observed, four cases have been selected. Each case correspond to one of the four seasons for 9, 12 and 15 UTC in each case.

The main inputs required by the LibRadtran software were describe in the previous chapters. The values for the main parameters (TOZ and aerosols) were obtained from the CAMS reanalysis data set for the selected cases. The measurements and the simulations were compared using a self programmed Python 3 script. This script reads the the TOZ and aerosols values from the CAMS reanalysis data set and creates the models input file. After that, it runs the LibRadtran software using the created input file. At last it reads the output files and creates the graphics and calculates the UVIs.

The CAMS reanalysis data was used for a precise estimation of the total ozone column, the solar zenith angle, and the calculations of the Ångström coefficients using the AOD<sub>469</sub> and AOD<sub>865</sub>. The values of these variables were obtained for the closest grid box available. A complete description of all the inputs for the simulations and the source from where they were obtained, are presented in Table 4.1.

## 4.2 Results

All the irradiances plots shown in this chapter, show as a thicker green curve, the Erythema Action Spectrum. This curve is illustrated in all the plots, in order to illustrate which range of the spectrum produces the strongest influence in the UVI.

The simulations for a case during the springtime were performed for the 21st of April. The estimated TOZ had a value of around 317 DU and the SZA was about  $40^{\circ}$  at 12 UTC. The results of the simulations and the measurements of the instrument located in Melpitz, are illustrated in Figure 4.1, where the plots correspond to 9, 12, 15 UTC from the top to the bottom respectively. Not only is the physical irradiance in  $W\ m^{-2}$  presented, but also the erythema weighted irradiances in  $W\ m^{-2}$  are illustrated in this figure for a better comparison between the simulations and the measurements.

Table 4.1: Set-up parameters and assumptions for comparing RT simulations with the measurements in Melpitz.

UV (280-400 nm) Resolution	0.1 nm
Time	Specific Date for Case of Study
RTE Solver	DISORT
Number of Streams	16
TOZ	Obtained from CAMS
SZA	Obtained from CAMS
Surface Albedo	0
Wavelengths Range	280-400 nm
Molecular Absorption Parametrization	REPTRAN
Angström Coefficients	Calculated from CAMS

The second case was in the summertime (26th of July, 2019). In this case, the sun is in a higher elevation compared to the first case. The results for this day are shown in Figure 4.2.

The last two cases correspond to the fall- and winter seasons respectively. These are presented in Figure 4.3 for the fall and Figure 4.4 for the winter. In the winter case, only two times a day at 9 and 12 UTC were possible to simulate, since the position of the sun at the 15 UTC was too low for the plane-parallel approximation. The plane-parallel solver usually neglects the curvature of the Earth and is a good approximation for SZAs lower than about 70° (Dahlback and Stamnes, 1991). In this case, only the SZA greater than 80° were not possible. The ones between 70° and 80° correlate to the rest of the cases shown in this section.

The results for all the cases are shown in table 4.2. These results show that when the sun is at higher elevation, the amount of the solar irradiance that reaches the surface is larger. This can be clearly seen in Table 4.2, where the parameters values obtained from the CAMS data, the results of the UVI calculations, and the absolute differences between the simulated and the observed UVIs are shown. Not only is the difference between the two UVIs are introduced in the table, but the linear correlation between the two irradiances was also calculated for each case. The calculations of the simulations were estimated using the Eq. 2.2, while the ones from the spectroradiometer, are taken directly from the NetCDF files obtained and proceed from the TROPOS Institute.

The TOZ had similar values in the spring- and summer cases with a value around 317 DU. The TOZ was between 262 and 268 DU during the fall- and winter days selected for this study. This corresponds to the mean curve of the period 2013-2018 shown in figure 2.4.

Table 4.2: Results of RT simulations, and Melpitz's measurements for case studies.

Time [UTC]	SZA [°]	TOZ [DU]	UVI Simulations [-]	UVI Melpitz [-]	Absolute Difference [-]	Linear Correlation
21/04/19 9	47.35	316.54	4.057	3.928	0.129	0.90
21/04/19 12	40.41	316.61	5.618	4.856	0.762	0.90
21/04/19 15	60.47	317.56	1.817	1.6	0.217	0.90
26/07/19 09	41.66	316.45	5.132	4.756	0.376	0.90
26/07/19 12	32.61	317.68	7.103	6.27	0.833	0.90
26/07/19 15	53.44	319	2.858	2.502	0.356	0.90
12/10/19 09	63.7	268.49	1.825	1.657	0.168	0.90
12/10/19 12	59.88	262.59	2.573	2.082	0.491	0.90
12/10/19 15	78	260.2	0.353	0.267	0.086	0.91
05/12/19 09	78.14	262.21	0.363	0.337	0.026	0.91
05/12/19 12	74.45	268.15	0.59	0.505	0.086	0.91

As a first impression of the figures shown in this section, the simulations do not differ strongly from the measurements which take place in Melpitz. In all the cases, the absolute differences on the UVIs occur at 12 UTC, with a difference around 0.8. The largest absolute difference occurs in the summer time, which was expected since the irradiance is stronger for that time of the year. However, that the differences between the UVIs are bigger at that time (see Figure 4.5), the linear correlation from the

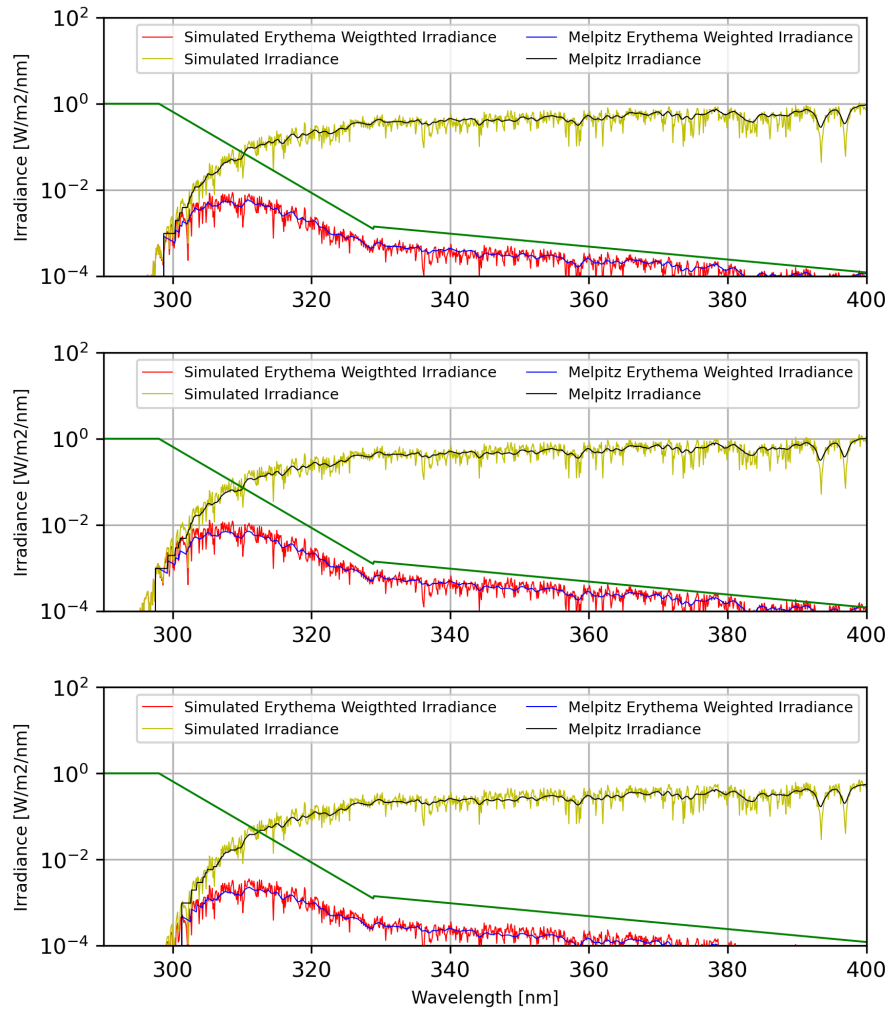


Figure 4.1: UV irradiance measured in Melpitz (black curve) and the erythema weighted irradiance (blue curve) compare with the UV irradiance simulated (yellow curve) and erythema weighted irradiance simulated (red curve) for the 21-04-2019 at 9 (top), 12 (center) and 15 (bottom) UTC.

irradiances are very similar in all the cases (see the plots for the summer day in the Appendix). All the simulations have a linear correlation of at least 90%.

The main difference to note is that for all the simulated cases, the UVI estimated from the RT modelling was greater than the one obtained from the spectroradiometer measurements. One of the reasons for this may be that, for the shortest wavelength, the measured irradiance has a value of zero. While the simulated irradiance has non-zero values for the same wavelengths. As it was mentioned in Chapter 2, the shortest wavelengths produce a big influence in the calculations of the UVI, when the irradiance is weighed with the erythema spectrum. The importance of the influence of the shortest wavelengths has been tested for this case (not shown), and the correction of this produce a decrease of the UVI calculated from the simulation of about 0.3. For a clearer understanding of these situations, the irradiance of both methods are presented for the summer case in Figure 4.5. Here it can be seen that both the irradiances do not differ strongly.

The main difference is how smooth the observed curve is in comparison to the noisy simulated one. The distribution of the simulated irradiance is associated to the precision of the model.

The problem with the differences between the UVI's can also be related to meteorological assumptions made for the simulations. Especially the fact that a standard atmosphere (US-standard) was used for the simulations. With this assumption, the main meteorological variables were defined from the model's atmospheric constituent profiles which was created in 1976. For a further and more precise analysis, all the model set-ups which were assumed from the available model inputs, could be created using the CAMS reanalysis data and correlated with the results of this thesis.

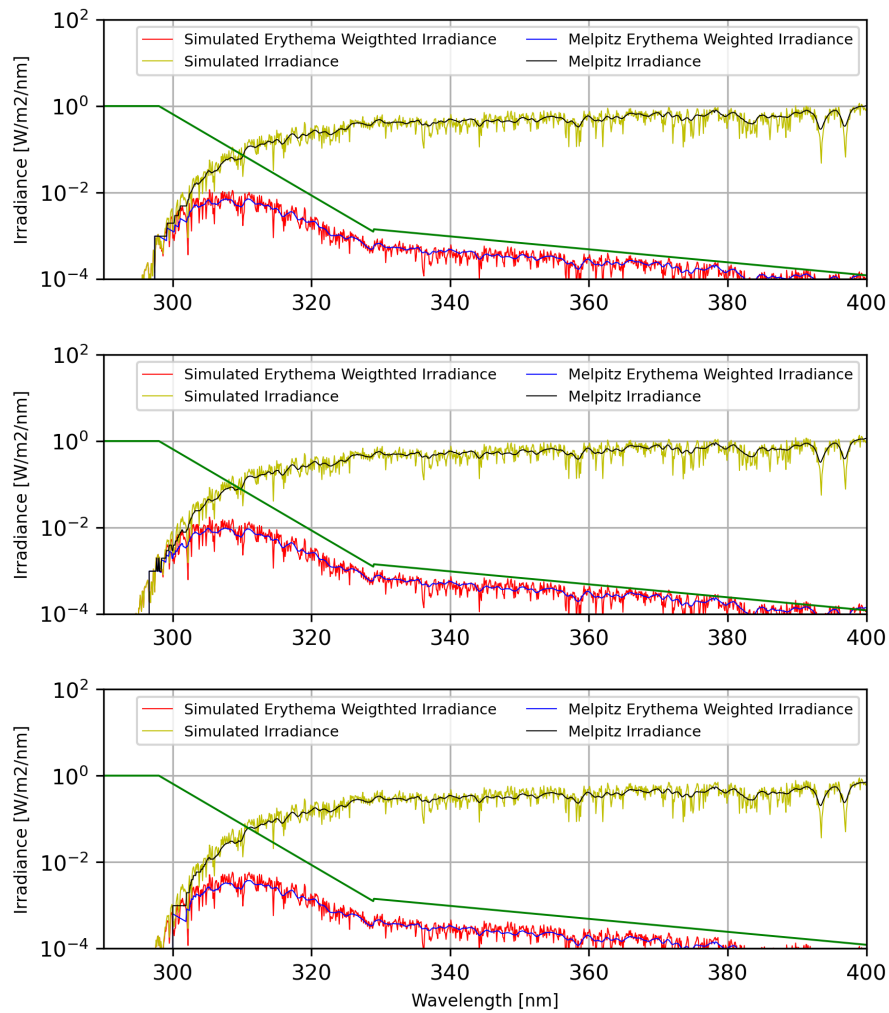


Figure 4.2: UV irradiance measured in Melpitz (black curve) and the erythema weighted irradiance (blue curve) compare with the UV irradiance simulated (yellow curve) and erythema weighted irradiance simulated (red curve) for the 26-07-2019 at 9 (top), 12 (center) and 15 (bottom) UTC.

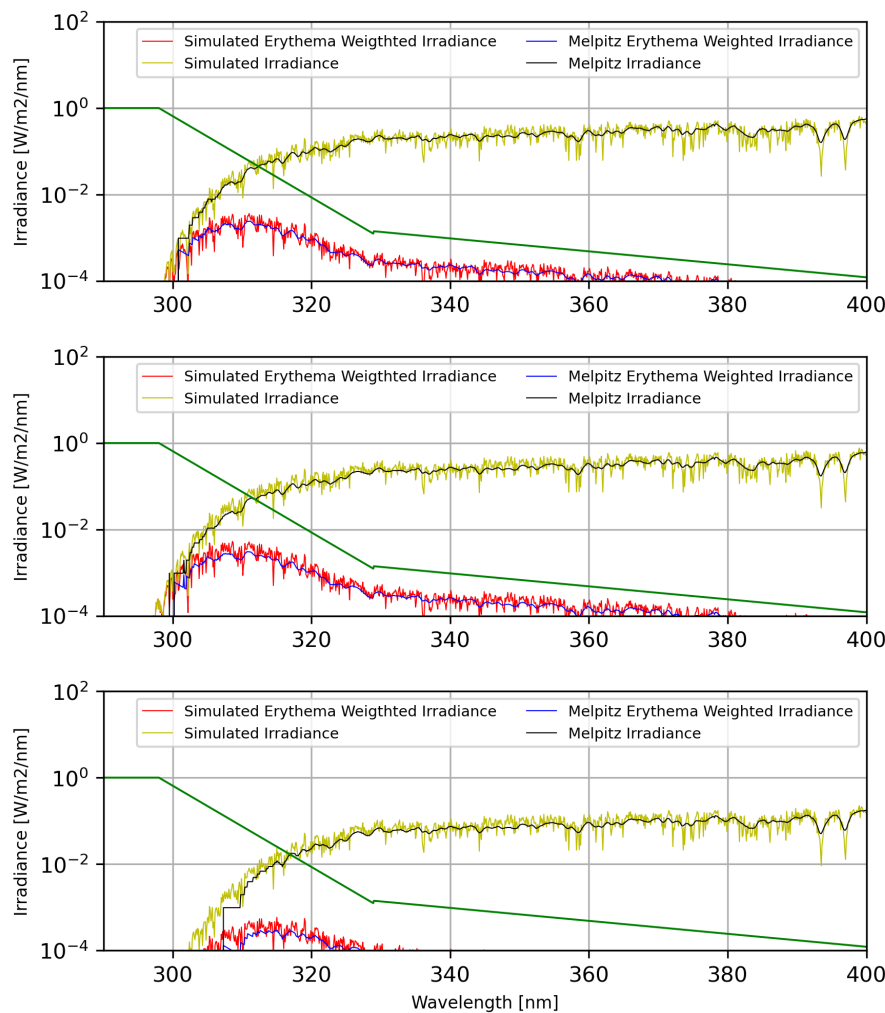


Figure 4.3: UV irradiance measured in Melpitz (black curve) and the erythema weighted irradiance (blue curve) compare with the UV irradiance simulated (yellow curve) and erythema weighted irradiance simulated (red curve) for the 12-10-2019 at 9 (top), 12 (center) and 15 (bottom) UTC.

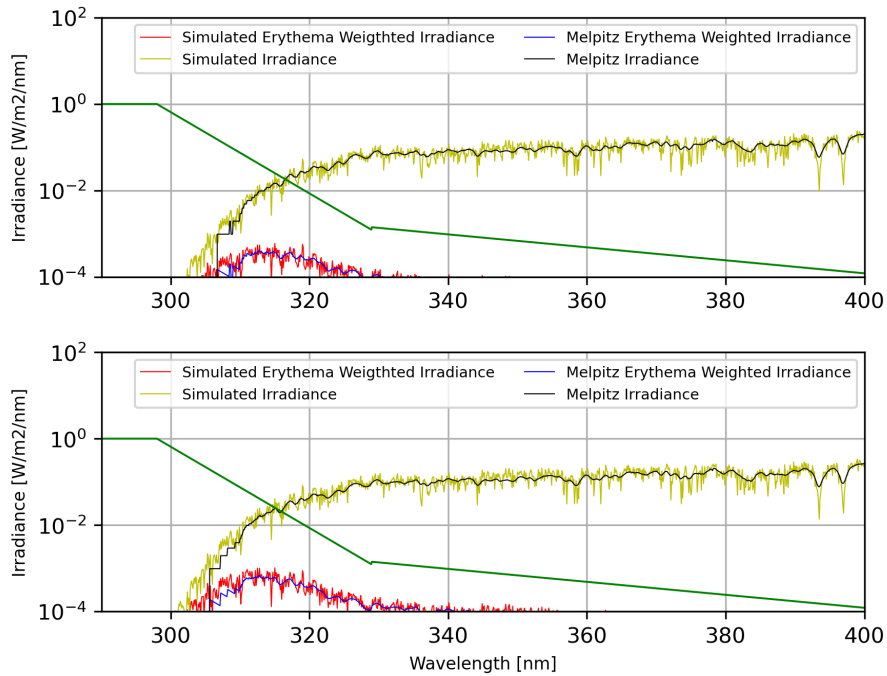


Figure 4.4: UV irradiance measured in Melpitz (black curve) and the erythema weighted irradiance (blue curve) compare with the UV irradiance simulated (yellow curve) and erythema weighted irradiance simulated (red curve) for the 05-12-2019 at 9 (top), 12 (bottom) UTC.

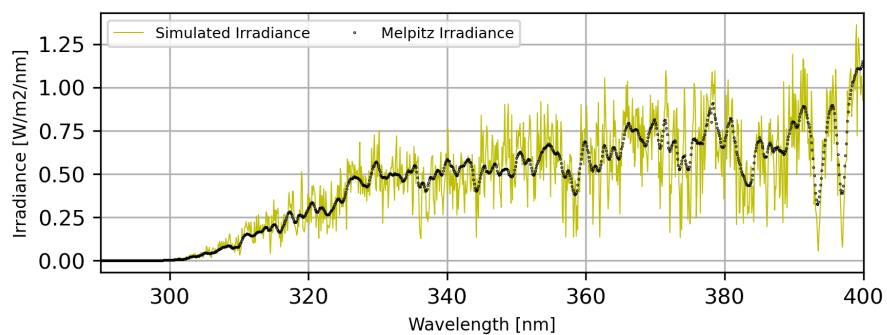


Figure 4.5: Simulated irradiance (yellow curve) and observed irradiance (black dots) for the 26/07/2019 at 12 UTC

# Chapter 5

# Conclusion and Outlook

This thesis presented a first analysis of the observations from the new spectroradiometer installed at 2018 for the meteorological station in Melpitz, Germany. This analysis consisted of the development of a RT modelling set up using the LibRadtran software. In the first two chapters, all the required factors for the UVI estimation were presented, as well as a detailed description of the reasons for the chosen software and the CAMS data set. The CAMS reanalysis data set was selected since it provides a precise description of the meteorological conditions for the parameters of interest. At the same time, it opens the possibility for a further development for using the CAMS forecast data, to create a modelling tool for a forecast of the UVI for the Melpitz station.

In Chapter 3, two sensitivity studies were presented. The first one determined which of the available molecular absorption parametrizations introduced the lowest level of uncertainty in the simulations. For this, two SZAs were used to determine if the simulations present a greater discrepancy with different values of this factor. The second sensitivity study looked at how the main parameters for the UVI estimation impact on the simulations.

Finally, a comparison between the RT modelling and the observations for a selected number of cases was shown in order to test its radiative closure. Not only was the precision of the RT simulations analyzed, but also the processing-time required for them was taken into consideration.

After these analyses, this chapter summarizes the main results and provides recommendations for future studies in this area of work.

## 5.1 Conclusions

### Sensitivity study

The results from Chapter 3 are presented here for both sensitivity studies. The objectives of those studies was to determinate the best available set-up for the RT modelling and to corroborate the impact of the influential factor for the UVI estimation with the literature.

- Three molecular absorption parametrizations (REPTRAN, CRS and LOWTRAN) available in the LibRadtran software using a plane-parallel approximation were tested. The REPTRAN parametrization was chosen since it seems to be the most precise, even though it required the largest processing-time. The processing-time required in this case was about 15 seconds per simulation. In case that a large number of simulations need to be performed, the *twostreams* solver could be used. In that case the UVI would be overestimated by the RT simulations. Even though it is the most precise, the differences between the three MAPs do not seem to be significantly different to rule out the other two in case a faster processing is required.
- During the molecular absorption parametrizations sensitivity study, two SZAs were used to determine if the differences caused by this parameter. The simulations seem to present a greater difference when the SZA was  $30^\circ$  (0.8) than in the  $60^\circ$  case (0.4). Those absolute differences correspond to the comparison between LOWTRAN and REPTRAN. The results from the CRS simulations were closer to the REPTRAN cases, but they have larger irradiance than the REPTRAN simulations.

- The second sensitivity study consisted in analyzing three influential factors for the solar radiation in the UV spectrum range. Those were TOZ, surface albedo and the total amount of aerosol. They were tested separately, using the same reference conditions for each case, to show how these variables affect the UVI calculations.
- As expected, the TOZ was proven to be the factor that introduces the greatest uncertainty in the UVI estimations. The main differences occur in the UV-B spectrum. The more TOZ, the less irradiance reaches the surface. Therefore, the lowest UVI was estimated when the TOZ=365 DU with a difference of about 10 % from the reference case (TOZ=335 DU).
- In the case of the surface albedo, the simulated irradiances do not seem to differ greatly. The main difference was that the reference irradiance curve was displaced in the y-axis. When the surface albedo was at its minimum (surface albedo= 0), the UVI was also at its minimum (UVI=1.74). An other aspect to note is that the surface albedo introduces the smallest uncertainty of all the studied factors.
- The last parameter studied was the AOD(550 nm). For this, the Ångström coefficient applied value was defined as a fix value, and the AOD<sub>550</sub> values were changed for each simulation. The results shown that when the atmosphere has a larger AOD, the irradiance that reaches the surface becomes more diffuse and the UVI is less intense.

### Comparison of Simulations with Observations

In Chapter 5, the radiative closure between the simulations and the observation was tested. The REPTRAN parametrization was used for those simulations. Four cases were selected for this part. Each case corresponded to one moment of a different season during 2019 and they presented clear-sky conditions for most of the day. That aspect was evaluated using SEVIRI satellite images. TOZ, SZA and aerosol were determined using the CAMS reanalysis data set available for the selected cases at closest grid box to the meteorological station. All the cases studied were compared with the observations at Melpitz for 9, 12 and 15 UTC. For the winter case (05/12/2019), only the 9 and 12 UTC times were available for comparing with this form of analysis. The main results of this comparison are described here.

- As a first impression, the simulations seem to match the observations. The UVI, the absolute difference between the UVIs and the linear correlation between the simulated and the observed irradiances were also calculated. All the cases presented almost a 90% of linear correlations between the simulated and observed spectral irradiances.
- The RT simulations are noisier than the measurements in all the cases. This is related to the optical bandwidth of the BTS2048-UV-S-WP spectroradiometer (0.8 nm). This could be analyzed in more detail by smoothing the simulated irradiance's curves were smoothed. This would also help to determinate if the specifications of the instrument agree with the manufacturer's descriptions. At the same time, if that aspect would be corrected, the linear correlation between the measured and observed irradiances should be closer to 1.
- Another aspect to highlight is that there appears to be a difference for the shortest wavelengths of the spectrum. The simulations present non-zero irradiance values where the instrument measures zero irradiance. Since the erythema action spectrum presents its maximum for those wavelengths, those differences increase the absolute difference between both UVIs. This difference was analyzed for the summertime day at 12 UTC, changing the non-zero values to zero as it was measured in Melpitz. In that case, the absolute difference between the UVIs was 0.3.
- All the estimated UVIs from the RT simulations have larger values than the observed ones. The largest relative differences of the UVIs occurred at 12 UTC for all the days. This corresponds to the highest elevation of the sun simulated each day. The maximal difference occurs in the summer case with an absolute discrepancy of 0.833, where the simulations over-estimates the UVI obtained from Melpitz.

- A possible explanation of the differences could be related to some of the meteorological assumptions (aerosols, albedo, etc) that were made for the RT simulations.

## 5.2 Outlook

It can be concluded that, despite the differences in all the cases between the simulations and the observation, that the simulations agreed relatively well with the instrumental measurements. However, more cases should be analyzed, in order to be able to confirm these results. The main effects of some of the most influential parameters agreed with the findings of several authors. A more detailed analysis of the impact of aerosols on the UVI, should be performed in a further study, to determine how the characteristics of aerosol impact on the UVI. Regarding the RT simulations, a more detailed set-up should be produced and tested to see if it is possible to reduce the error of the simulations. A current and more precise atmospheric file should decrease the absolute differences.

On the other hand, a comparison of the used instrument with another instrument, could bring more clarity on the differences that were seen at the shortest wavelengths. Also, an analysis of the spectral curve of the simulated irradiance could help clarify if the differences between the irradiances is related to the precision of the instrument or to the RT simulations.

This work could be the first step towards an operational application modelled forecast using this RT simulation's set up. This idea was taken into consideration as the CAMS reanalysis data set was chosen, since the ECMWF also produces CAMS forecast data. That data set could be used to determinate the value of TOZ and aerosols and use them to produce a forecast for that station. This could be used as comparison measure with the forecast that is produced for the UVI in Melpitz by the BfS.

# Bibliography

- Alfaro Lozano, L., Llacza Rodríguez, A., and Sánchez Ccoyllo, O. (2016). Pronóstico con cobertura nacional del índice de radiación solar ultravioleta.
- Allaart, M., van Weele, M., Fortuin, P., and Kelder, H. (2004). An empirical model to predict the uv-index based on solar zenith angles and total ozone. *Meteorological Applications: A journal of forecasting, practical applications, training techniques and modelling*, 11(1):59–65.
- Anderson, G. P., Clough, S. A., Kneizys, F., Chetwynd, J. H., and Shettle, E. P. (1986). Afgl atmospheric consituent profiles (0.120 km). Technical report, AIR FORCE GEOPHYSICS LAB HANSCOM AFB MA.
- Ångström, A. (1961). Techniques of determinig the turbidity of the atmosphere. *Tellus*, 13(2):214–223.
- Badosa, J. (2002). Mesures d'irradiancia eritematica a catalunya vs. modelitzacions per cels serens a partir de la columna d'ozó d'ep/toms (erythemal irradiance measurements in catalonia vs. modelling for clear skies using the ozone column from ep/toms). *Minor thesis, Dept. of Physics, University of Girona*.
- Badosa, J. and Weele, M. v. (2002). *Effects of aerosols on UV-index*. KNMI.
- Buras, R., Dowling, T., and Emde, C. (2011). New secondary-scattering correction in disort with increased efficiency for forward scattering. *Journal of Quantitative Spectroscopy and Radiative Transfer*, 112(12):2028–2034.
- Chadyšiene, R. and Girgždys, A. (2008). Ultraviolet radiation albedo of natural surfaces. *Journal of environmental engineering and landscape management*, 16(2):83–88.
- Čížková, K., Láska, K., Metelka, L., and Staněk, M. (2018). Reconstruction and analysis of erythemal uv radiation time series from hradeč králové (czech republic) over the past 50 years. *Atmospheric Chemistry and Physics*, 18(3):1805–1818.
- Dahlback, A. and Stamnes, K. (1991). A new spherical model for computing the radiation field available for photolysis and heating at twilight. *Planetary and Space Science*, 39(5):671–683.
- Emde, C., Buras-Schnell, R., Kylling, A., Mayer, B., Gasteiger, J., Hamann, U., Kylling, J., Richter, B., Pause, C., Dowling, T., et al. (2016). The libradtran software package for radiative transfer calculations (version 2.0. 1). *Geoscientific Model Development*, 9(5):1647–1672.
- Fioletov, V., McArthur, L., Mathews, T., and Marrett, L. (2009). On the relationship between erythemal and vitamin d action spectrum weighted ultraviolet radiation. *Journal of Photochemistry and Photobiology B: Biology*, 95(1):9–16.
- Fioletov, V. E., Kerr, J. B., and Fergusson, A. (2010). The uv index: definition, distribution and factors affecting it. *Canadian journal of public health = Revue canadienne de sante publique*, 101 4:15–9.
- Gasteiger, J., Emde, C., Mayer, B., Buras, R., Buehler, S., and Lemke, O. (2014). Representative wavelengths absorption parameterization applied to satellite channels and spectral bands. *Journal of Quantitative Spectroscopy and Radiative Transfer*, 148:99–115.

- Inness, A., Ades, M., Agustí-Panareda, A., Barré, J., Benedictow, A., Blechschmidt, A.-M., Dominguez, J. J., Engelen, R., Eskes, H., Flemming, J., Huijnen, V., Jones, L., Kipling, Z., Massart, S., Parrington, M., Peuch, V.-H., Razinger, M., Remy, S., Schulz, M., and Suttie, M. (2019). The cams reanalysis of atmospheric composition. *Atmospheric Chemistry and Physics*, 19(6):3515–3556.
- Kylling, A. (1993). Radiation transport in cloudy and aerosol loaded atmospheres. In *Atmospheric Radiation*, volume 2049, pages 78–89. International Society for Optics and Photonics.
- Mayer, B. and Kylling, A. (2005). The libradtran software package for radiative transfer calculations—description and examples of use.
- McKenzie, R., Paulin, K., and Madronich, S. (1998). Effects of snow cover on uv irradiance and surface albedo: A case study. *Journal of Geophysical Research: Atmospheres*, 103(D22):28785–28792.
- McKinlay, A. (1987). A reference action spectrum for ultraviolet erythema in human skin. *CIE journal*, 6:17–22.
- Renaud, A., Staehelin, J., Fröhlich, C., Philipona, R., and Heimo, A. (2000). Influence of snow and clouds on erythemal uv radiation: Analysis of swiss measurements and comparison with models. *Journal of Geophysical Research: Atmospheres*, 105(D4):4961–4969.
- Sabburg, J. and Wong, J. (2000). The effect of clouds on enhancing uvb irradiance at the earth's surface: a one year study. *Geophysical Research Letters*, 27(20):3337–3340.
- Schmalwieser, A. W., Gröbner, J., Blumthaler, M., Klotz, B., De Backer, H., Bolsée, D., Werner, R., Tomsic, D., Metelka, L., Eriksen, P., et al. (2017). Uv index monitoring in europe. *Photochemical & Photobiological Sciences*, 16(9):1349–1370.
- Stamnes, K., Tsay, S.-C., Wiscombe, W., and Laszlo, I. (2000). Disort, a general-purpose fortran program for discrete-ordinate-method radiative transfer in scattering and emitting layered media: documentation of methodology.
- Van Weele, M., Martin, T., Blumthaler, M., Brogniez, C., Den Outer, P., Engelsen, O., Lenoble, J., Mayer, B., Pfister, G., Ruggaber, A., et al. (2000). From model intercomparison toward benchmark uv spectra for six real atmospheric cases. *Journal of Geophysical Research: Atmospheres*, 105(D4):4915–4925.
- WHO (1995). *Global solar UV index: a practical guide*. World Health Organization (WHO) and International Commission on Non-Ionizing Radiation Protection and others.

# List of Figures

1.1	The measuring stations network from the Federal Office for Radiation Protection in Germany, where Melpitz is marked with a red dot (taken from <a href="http://www.bfs.de">www.bfs.de</a> ) . . . . .	2
1.2	UVI color scale and international category of exhibition (Source: WHO (1995)) . . . . .	2
2.1	Transmittance simulated in LibRadtran for the 23/08/2019 at 12 UTC, solar zenith angle obtained from CAMS reanalysis data(right). Spectral irradiance simulated for the UV range for the 23/08/2019 at 12 UTC, solar zenith angle obtained from CAMS reanalysis data(left) . . . . .	5
2.2	Meteorological station located in Melpitz, Germany, which is a part of the solar UV-network from the Federal Office for Radiation Protection (Source: Leibnitz-Institute for Tropospheric research) . . . . .	5
2.3	Representation of the global irradiance that reach the surface on a summer day (blue curve), erythema action spectrum (red curve), vitamin D action spectrum (green curve) and ozone absorption (purple curve) (Fioletov et al., 2009) . . . . .	7
2.4	Total Ozone Column statistical distribution (left) and time series distribution of the mean TOZ in the period 2013-2018 (right). Produced via CAMS Reanalysis for Melpitz.	8
2.5	Statistical distribution for aerosol optical depth at 469 nm (left) and 865 nm (right); plotted from CAMS Reanalysis for Melpitz. . . . .	9
2.6	Structure of the <i>uvspec</i> radiative transfer model (Emde et al., 2016) . . . . .	11
3.1	Erythema weighted irradiances for sensitivity study for the effects of TOZ on the RT simulations using <i>UVSPEC</i> model in the UV spectrum. . . . .	15
3.2	Erythema weighted irradiances for sensitivity study for the impact of surface albedo on the RT simulations using <i>UVSPEC</i> model in the UV spectrum. . . . .	16
3.3	Erythema weighted irradiances for sensitivity study for the effects of aerosols on the RT simulations using <i>UVSPEC</i> model in the UV spectrum. . . . .	18
4.1	UV irradiance measured in Melpitz (black curve) and the erythema weighted irradiance (blue curve) compare with the UV irradiance simulated (yellow curve) and erythema weighted irradiance simulated (red curve) for the 21-04-2019 at 9 (top), 12 (center) and 15 (bottom) UTC. . . . .	21
4.2	UV irradiance measured in Melpitz (black curve) and the erythema weighted irradiance (blue curve) compare with the UV irradiance simulated (yellow curve) and erythema weighted irradiance simulated (red curve) for the 26-07-2019 at 9 (top), 12 (center) and 15 (bottom) UTC. . . . .	22
4.3	UV irradiance measured in Melpitz (black curve) and the erythema weighted irradiance (blue curve) compare with the UV irradiance simulated (yellow curve) and erythema weighted irradiance simulated (red curve) for the 12-10-2019 at 9 (top), 12 (center) and 15 (bottom) UTC. . . . .	23
4.4	UV irradiance measured in Melpitz (black curve) and the erythema weighted irradiance (blue curve) compare with the UV irradiance simulated (yellow curve) and erythema weighted irradiance simulated (red curve) for the 05-12-2019 at 9 (top), 12 (bottom) UTC. . . . .	24

4.5	Simulated irradiance (yellow curve) and observed irradiance (black dots) for the 26/07/2019 at 12 UTC . . . . .	24
1	Aerosol optical depth's Time Series for the 2013-2018 period. Data plotted from the CAMS reanalysis data set. . . . .	vi
2	Total Ozone Column's Time Series (left) and Histograms for each season (right) for the 2013-2018 period . Data plotted from the CAMS reanalysis data set. . . . .	vi
3	UV irradiace simulations for Sensitivity study I. . . . .	vii
4	Simulated and observed irradiances for the 21/04/2019 (top), 12/10/2019 (center) and 05/12/2019 at 12 UTC for each day . . . . .	viii
5	Correlation between the simulations and the observation for the 26/07/2019 at 9 (top), 12 (center) and 15 (bottom) UTC. . . . .	ix

# List of Tables

3.1	Set-up parameters and assumptions for model configuration's inputs sensitivity study.	13
3.2	Results obtained for model configuration's inputs sensitivity study. . . . .	14
3.3	Set-up parameters and assumptions for analyzing the effects of TOZ in the RT simulations.	15
3.4	Results of RT simulations to determine the effects of TOZ on the UV irradiance simulations. . . . .	15
3.5	Set-up parameters and assumptions for analyzing the effects of surface albedo in the RT simulations. . . . .	16
3.6	Results of RT simulations to determine the effects of surface albedo on the UV irradiance simulations. . . . .	17
3.7	Set-up parameters and assumptions for analyzing the effects of aerosols in the RT simulations. . . . .	17
3.8	Results of RT simulations to determine the effects of aerosols on the UV irradiance simulations. . . . .	17
4.1	Set-up parameters and assumptions for comparing RT simulations with the measurements in Melpitz. . . . .	20
4.2	Results of RT simulations, and Melpitz's measurements for case studies. . . . .	20

# Apendix

Here some extra graphics for the analysis of the CAMS data for the period of 2013-2018 (Figures 1 and 2), for the sensitivity study 3.1 (Figure 3) and of the case studies (Figures 4 and 5).

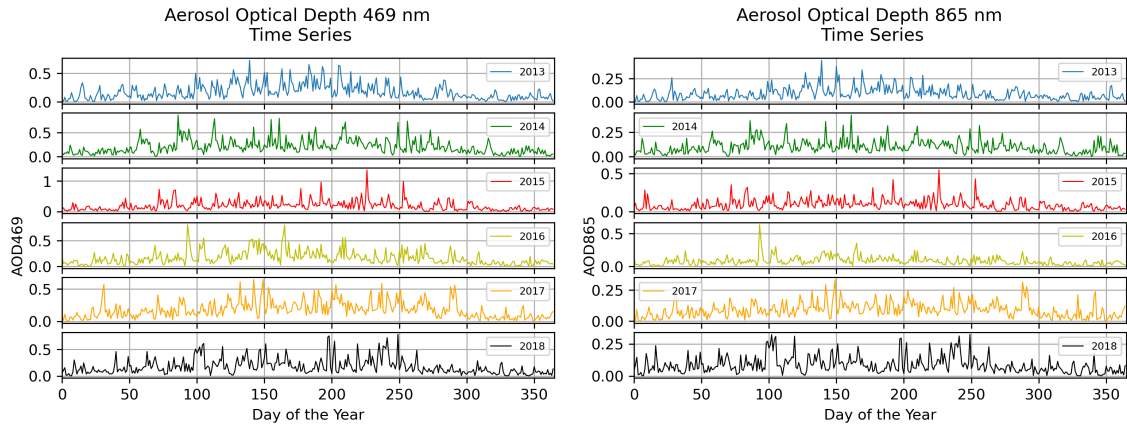


Figure 1: Aerosol optical depth's Time Series for the 2013-2018 period. Data plotted from the CAMS reanalysis data set.

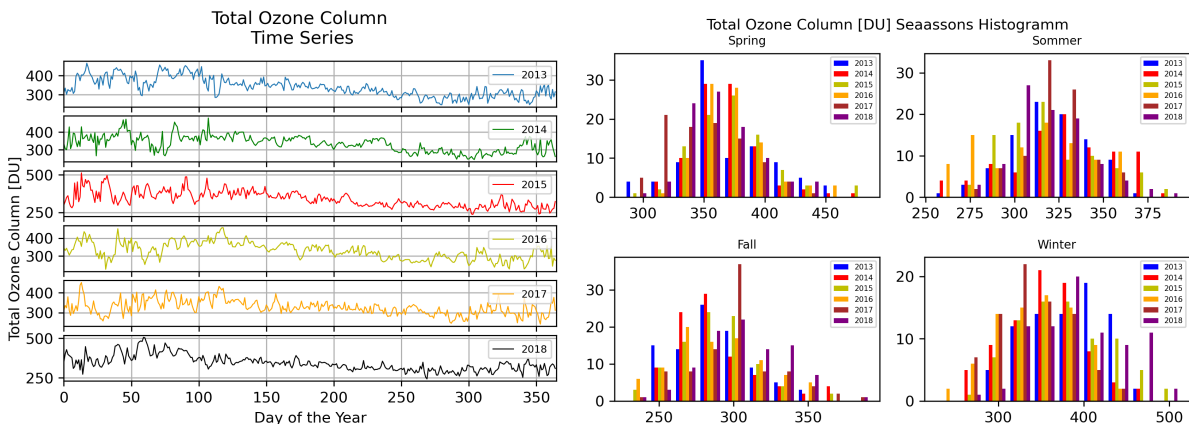


Figure 2: Total Ozone Column's Time Series (left) and Histograms for each season (right) for the 2013-2018 period . Data plotted from the CAMS reanalysis data set.

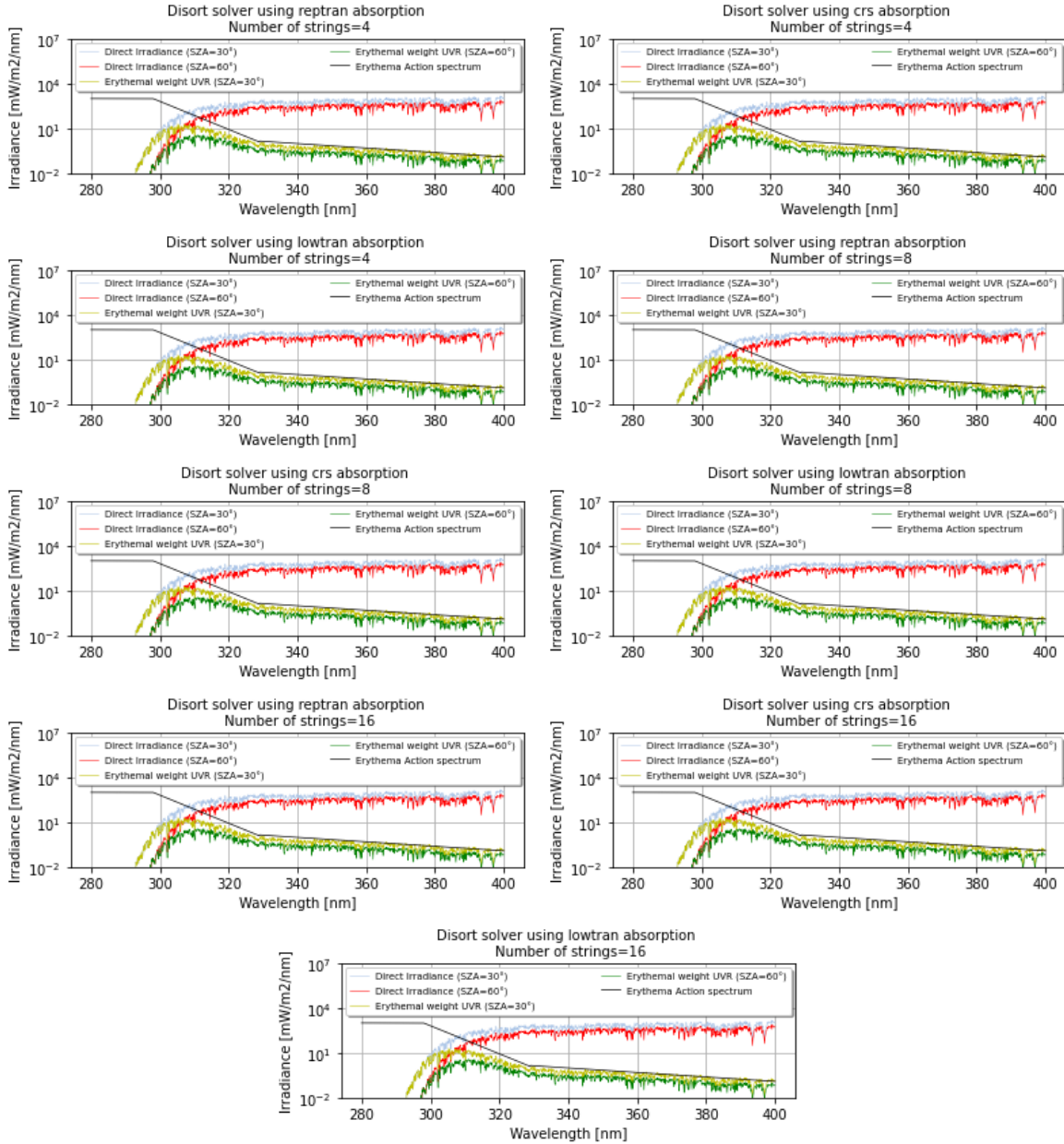


Figure 3: UV irradiace simulations for Sensitivity study I.

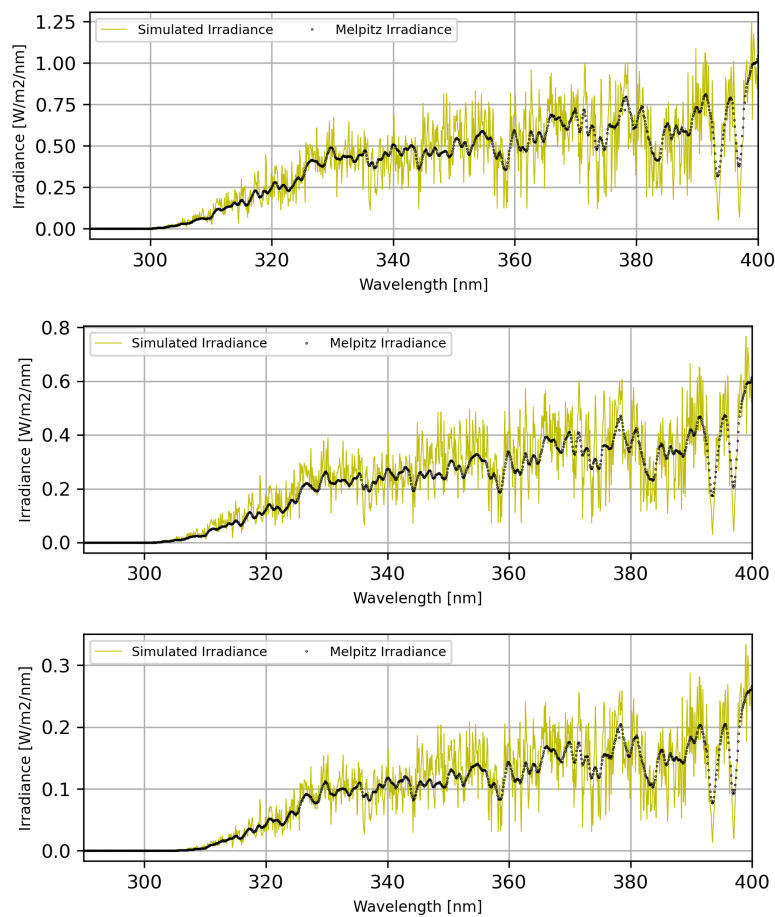


Figure 4: Simulated and observed irradiances for the 21/04/2019 (top), 12/10/2019 (center) and 05/12/2019 at 12 UTC for each day

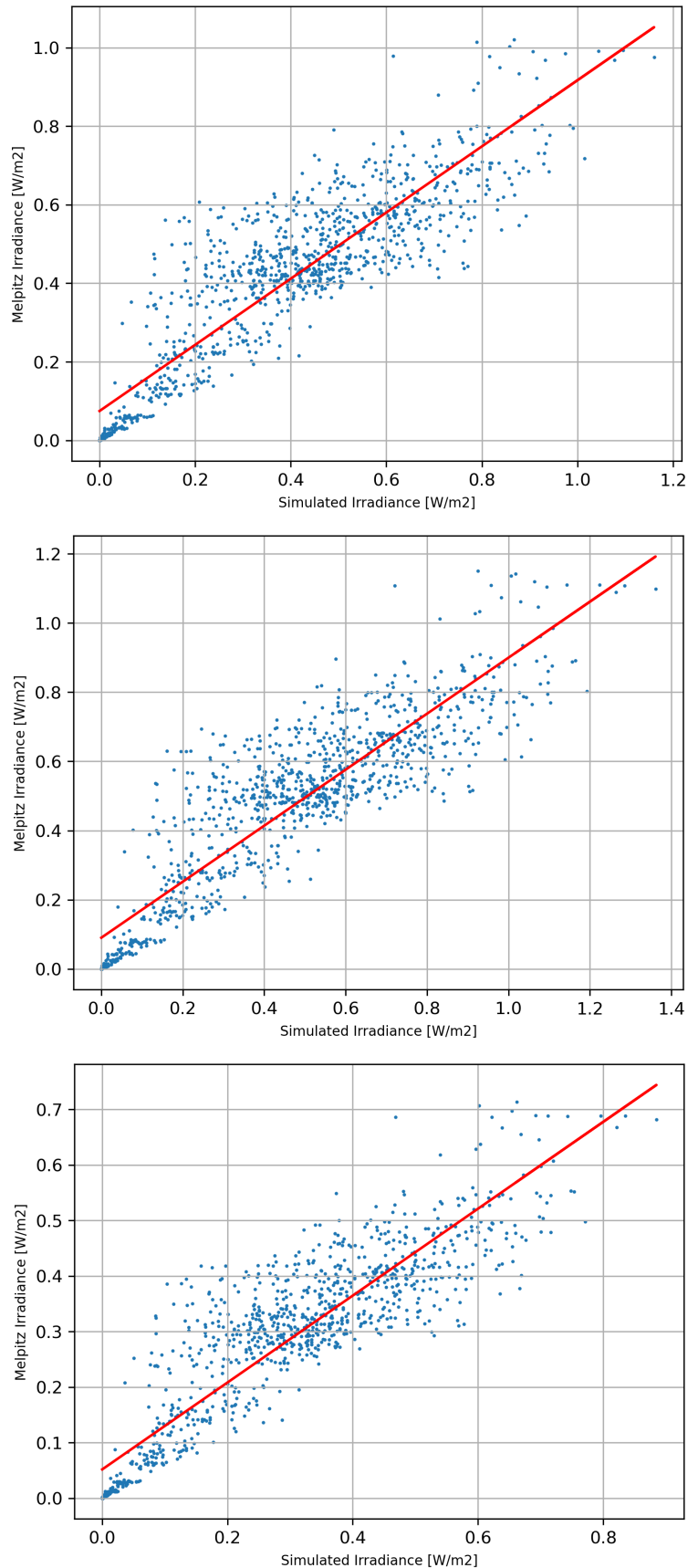


Figure 5: Correlation between the simulations and the observation for the 26/07/2019 at 9 (top), 12 (center) and 15 (bottom) UTC.



# Declaration

I hereby confirm that I will use the present work to obtain the academic degree Bachelor of Science independently and only using the specified sources and resources to have made. All quotes are marked as such. I confirm that this work has not yet been submitted elsewhere to obtain the degree "Bachelor of Science".

---

Nicolas Bayer

---

Date